



Chaotic transients in spatially extended systems

Tamás Tél^{a,*}, Ying-Cheng Lai^{b,c}^a *Institute for Theoretical Physics, Eötvös University, Pázmány P. s. 1/A, Budapest, H-1117, Hungary*^b *Department of Electrical Engineering, Arizona State University, Tempe, AZ 85287, USA*^c *Department of Physics and Astronomy, Arizona State University, Tempe, AZ 85287, USA*

Accepted 30 January 2008

Available online 13 February 2008

editor: I. Procaccia

Abstract

Different transient-chaos related phenomena of spatiotemporal systems are reviewed. Special attention is paid to cases where spatiotemporal chaos appears in the form of chaotic transients only. The asymptotic state is then spatially regular. In systems of completely different origins, ranging from fluid dynamics to chemistry and biology, the average lifetimes of these spatiotemporal transients are found, however, to grow rapidly with the system size, often in an exponential fashion. For sufficiently large spatial extension, the lifetime might turn out to be larger than any physically realizable time. There is increasing numerical and experimental evidence that in many systems such transients mask the real attractors. Attractors may then not be relevant to certain types of spatiotemporal chaos, or turbulence. The observable dynamics is governed typically by a high-dimensional chaotic saddle. We review the origin of exponential scaling of the transient lifetime with the system size, and compare this with a similar scaling with system parameters known in low-dimensional problems. The effect of weak noise on such supertransients is discussed. Different crisis phenomena of spatiotemporal systems are presented and fractal properties of the chaotic saddles underlying high-dimensional supertransients are discussed. The recent discovery according to which turbulence in pipe flows is a very long lasting transient sheds new light on chaotic transients in other spatially extended systems.

© 2008 Elsevier B.V. All rights reserved.

PACS: 05.45.-a

Keywords: Transient chaos; Spatiotemporal dynamical systems; Supertransients; Chaotic saddle; Turbulence; Pipe flow

Contents

1. Introduction.....	246
2. Basic characteristics of spatiotemporal chaos.....	247
2.1. Paradigmatic models	247
2.2. Phase spaces of spatiotemporal systems	248
2.3. Spatiotemporal intermittency	249

* Corresponding author. Tel.: +36 1 372 2524; fax: +36 1 372 2509.

E-mail addresses: tel@general.elte.hu (T. Tél), Ying-Cheng.Lai@asu.edu (Y.-C. Lai).URL: <http://www.chaos1.la.asu.edu/~yclai> (Y.-C. Lai).

3.	Supertransients in low-dimensional dynamical systems.....	250
3.1.	Unstable–unstable pair bifurcation and scaling of average transient lifetime.....	250
3.2.	A classical example.....	252
4.	Supertransients in spatially extended dynamical systems.....	252
4.1.	Transient chaos in coupled map lattices.....	252
4.2.	The origin of supertransient scaling.....	253
4.3.	Supertransients with exponentially long lifetimes in other systems.....	255
4.4.	Stable chaos.....	255
5.	Effect of noise on supertransients.....	256
5.1.	Low-dimensional systems.....	256
5.2.	Effect of noise and nonlocal coupling on supertransients in spatially extended dynamical systems.....	258
6.	Crises in spatiotemporal dynamical systems.....	260
6.1.	Supertransients preceding asymptotic spatiotemporal chaos.....	260
6.2.	Interior crises in spatially coherent chaotic systems.....	260
6.3.	Crises leading to fully developed spatiotemporal chaos.....	262
7.	Fractal properties of supertransients.....	264
7.1.	Partial dimension.....	264
7.2.	Application of general dimension formulae.....	266
7.3.	Dimension densities.....	267
8.	Turbulence in pipe flows.....	268
8.1.	Turbulence lifetime.....	268
8.2.	Other aspects of hydrodynamical supertransients.....	271
9.	Discussions.....	272
	Acknowledgements.....	273
	References.....	273

1. Introduction

Chaos is not restricted to systems without any spatial extension: it in fact occurs commonly in spatially extended dynamical systems [1–5] that are most typically described by nonlinear partial differential equations (PDEs). If the patterns generated by such a system change randomly in time, we speak of spatiotemporal chaos, which is then a kind of temporally chaotic pattern forming process. If, in addition, the patterns are also spatially irregular, we speak of fully developed spatiotemporal chaos. In principle, the phase space of the problem is infinitely dimensional. In practice, when a spatial discretization scheme is used to solve the PDE, or when measurements are made in a physical experiment with finite spatial resolution, the effective dimension of the phase space is not infinite but still high.

Transient chaos is common in dissipative spatiotemporal systems. The basic reason is that spatial coupling is typically diffusive, which prefers the neighboring sites to behave similarly (to synchronize). The asymptotic attractors are often temporally periodic ones, or even time-independent. It is the approach towards these attractors which is chaotic. In this sense, spatiotemporal chaos often collapses after some time, and a regular behavior then takes over.

A fundamental and physically significant characteristic of transient chaos in low-dimensional systems is its lifetime and the associated scaling laws [6,7]. This is also true for transient chaos in spatiotemporal dynamical systems. The basic feature that distinguishes a low-dimensional dynamical system from a spatially extended system is its size in space. Thus one is naturally interested in the scaling law of the transient lifetime, or the escape rate (the inverse of the lifetime), with the system size. If the lifetime increases rapidly with the system size, we speak of *supertransients*. An important physical example of supertransients is fluid dynamical turbulence in pipe flows. Here the well-known stationary laminar solution is the only asymptotic attractor, and the observed turbulent behavior appears to be a kind of transient chaos only. Motivated by this example, we shall sometimes call the fully developed chaotic behavior of other spatiotemporal systems “turbulent.”

In systems exhibiting supertransients, a general picture emerges: In a large system, it is not possible to determine whether the observed “turbulence” is transient unless an asymptotic time regime is reached. If the transient time is much longer than any physically realizable time, the system is effectively “turbulent,” regardless of the nature of the asymptotic attractor. The transients mask in this case the real attractor, and pose a fundamental difficulty for observing the asymptotic state of the system. In this sense, attractors are irrelevant to “turbulence.” Supertransients

are thus perhaps the most surprising applications of the concept of transient chaos to spatially extended dynamical systems.

Chaotic transients whose lifetimes grow exponentially or even much faster as some system parameter passes through a critical point were first discovered in low-dimensional dynamical systems by Grebogi, Ott and Yorke [8]. In such a case supertransients are triggered by an unstable–unstable pair bifurcation that signifies the coalescence of two unstable periodic orbits having different unstable dimensions: one in a chaotic attractor and another on the basin boundary. Because of the difference in the unstable dimension, “channels” through which trajectories can escape from the original chaotic attractor typically are low-dimensional (as compared with the phase–space dimension of the system itself). The chaotic nature of the original attractor stipulates that the channels be extremely “thin,” leading to a supertransient. Supertransients in low-dimensional systems may provide useful insights into the mechanism leading to extremely long transients in spatially extended systems.

This brief review is organized as follows. In Section 2, we introduce several paradigmatic models of spatially extended dynamical systems and describe their basic characteristics. In Section 3, we focus on supertransients in low-dimensional systems and sketch the analysis that leads to the characteristic scaling law in terms of parameter variations. In Section 4, we discuss supertransients in different models of spatially extended systems, and different types of scaling laws with the system size are derived. In Section 5, we investigate the effect of noise on supertransients, both for low-dimensional and spatiotemporal dynamical systems. In particular, in low dimensions recent analytic results derived from the theory of Langevin dynamics will be described. In Section 6, we describe the dynamical phenomenon of external and internal crises in spatially extended systems. Section 7 is devoted to the fractal properties of supertransients and explicit expressions are found. Turbulence in pipe flows, which represents an important physical situation where supertransients can be observed experimentally, is discussed in Section 8. Finally, a brief summary and outlook is presented in Section 9.

2. Basic characteristics of spatiotemporal chaos

2.1. Paradigmatic models

There are several classes of models of spatially extended systems ranging from physics to biology, exhibiting spatial patterns of complex time and space dependence. Comprehensive reviews of the dynamical aspects of such spatiotemporal patterns can be found in, e.g., Refs. [1–5]. Here we briefly summarize the basic models.

Coupled map lattices (CML), introduced by Kaneko [1], provide the simplest models for spatiotemporal dynamics of continuous variables. The attractive feature is that the local building blocks of the dynamics are in the form of low-dimensional maps f . They are coupled to their neighbors according to some rule with a coupling of strength ε . In this model, both time and space are discrete, but the dynamical variables are continuous. The dynamics does depend on the boundary conditions. Often periodic boundary conditions are taken, but absorbing boundary conditions have also been used. In one dimension, the typical form of a CML defined on N sites with diffusive local coupling is

$$x_{n+1}^i = (1 - \varepsilon)f(x_n^i) + \frac{\varepsilon}{2} \left[f(x_n^{i+1}) + f(x_n^{i-1}) \right], \quad i = 0, \dots, N - 1, \quad (1)$$

where x is the dynamical variable, and n and i denote discrete time and space, respectively. For periodic boundary conditions $x_n^0 = x_n^{N-1}$, while for absorbing boundary conditions we have $x_n^0 = x_n^{N-1} = 0$ for any time instant n . The size L of a CML can be identified as N , the number of sites.

In a *cellular automaton (CA)* [2] even the dynamical variable is discrete. By coarsening the x variable of a CML, the dynamics is mapped on that of a CA [9]. If, for example, the new variable is chosen to be 0 (1) for x smaller (larger) than a threshold, a two-state CA is obtained from (1). We therefore do not investigate the spatiotemporal dynamics of CAs separately.

The Kuramoto–Shivashinsky (KS) equation is a simple PDE exhibiting interesting spatiotemporal dynamics. It was derived to describe propagating patterns in plasmas, in chemistry and in cellular flames [3]. The KS equation governs the dynamics of a continuous scalar field $u(x, t)$ according to a nonlinear equation whose dimensionless form can be written as

$$\frac{\partial u}{\partial t} = -u \frac{\partial u}{\partial x} - \frac{\partial^2 u}{\partial x^2} - \frac{\partial^4 u}{\partial x^4}. \quad (2)$$

It is remarkable that there are no free parameters in the model and, hence, the system size L serves as the only control parameter. Alternatively, one can fix the size and, after appropriate rescaling, convert Eq. (2) to

$$\frac{\partial u}{\partial t} = -u \frac{\partial u}{\partial x} - \frac{\partial^2 u}{\partial x^2} - v \frac{\partial^4 u}{\partial x^4}, \quad (3)$$

where $v \sim L^2$ is a dimensionless parameter.

The complex Ginzburg–Landau (cGL) equation governs the spatiotemporal evolution of a complex field $\psi(\mathbf{r}, t)$. It is the normal form of spatiotemporal systems in the vicinity of Hopf bifurcations [3]. In the most commonly used two-dimensional version the cGL equation reads as

$$\frac{\partial \psi}{\partial t} = \mu \psi - (1 + i\alpha) \Delta \psi + (1 + i\beta) |\psi|^2 \psi, \quad (4)$$

where Δ denotes the Laplacian. The system has three dimensionless parameters: μ , α and β . When the dimensionless system size is fixed, the parameter μ carries the size dependence.

Reaction–diffusion (RD) equations describe the coupled dynamics of chemical concentrations, or interacting populations. Their general form for two concentrations $a(\mathbf{r}, t)$ and $b(\mathbf{r}, t)$ is

$$\frac{\partial a}{\partial t} = r_a(a, b) + \Delta a, \quad \frac{\partial b}{\partial t} = r_b(a, b) + \delta \Delta b. \quad (5)$$

Here functions r_a , r_b govern the nonlinear reaction equations in the homogeneous case, and the dimensionless parameter

$$\delta = D_b/D_a$$

is the ratio of the diffusion coefficients.

The Navier–Stokes (NS) equations describe the dynamics of the velocity and pressure fields, $\mathbf{v}(\mathbf{r}, t)$ and $p(\mathbf{r}, t)$, respectively, of a viscous fluid. For incompressible flows not subject to any external force their dimensionless form is

$$\frac{\partial \mathbf{v}}{\partial t} + \mathbf{v} \nabla \mathbf{v} = -\nabla p + \frac{1}{Re} \Delta \mathbf{v}, \quad \nabla \cdot \mathbf{v} = 0, \quad (6)$$

where Re is the Reynolds number. Note that there is no dynamical equation for the pressure. It is the incompressibility equation $\nabla \cdot \mathbf{v} = 0$ which provides a condition of self-consistency to make the pressure unique. The Reynolds number

$$Re = \frac{UD}{\nu} \quad (7)$$

is a basic dimensionless parameter, where U and D represent a characteristic velocity and length, respectively, and ν is the kinematic viscosity.

Figs. 1a and 1b presents a couple of typical complex patterns in spatiotemporal systems.

2.2. Phase spaces of spatiotemporal systems

The phase space of spatiotemporal systems is always high-dimensional. In a CML, it is spanned by all the variables x^i at different sites $i = 0, \dots, N - 1$. In a system described by nonlinear PDEs, the phase space is spanned by the set of all possible spatial distributions of the fields, compatible with a given boundary condition, which are infinite dimensional. In the KS and cGL equations, these are the function spaces $u(x)$ and $\psi(\mathbf{r})$, respectively. In RD problems and fluid dynamics two functions define the phase space, the set of all possible concentrations $a(\mathbf{r})$ and $b(\mathbf{r})$, and the set of all possible velocity and pressure fields, $\mathbf{v}(\mathbf{r})$ and $p(\mathbf{r})$, respectively. The form of the functions appearing here is basically determined by the boundary condition in question. In the NS problem, for example, all velocity fields should vanish on nonmoving walls, or take on the values of the velocities of the walls if they move.

A given spatial distribution of the field variable represents a point of the phase space. Any of them can be a possible initial condition. The time evolution of the system corresponds to a motion among different phase space points, and traces out a continuous curve emanating from the point representing the initial state. The time evolution is unique, and the phase space description is thus complete.

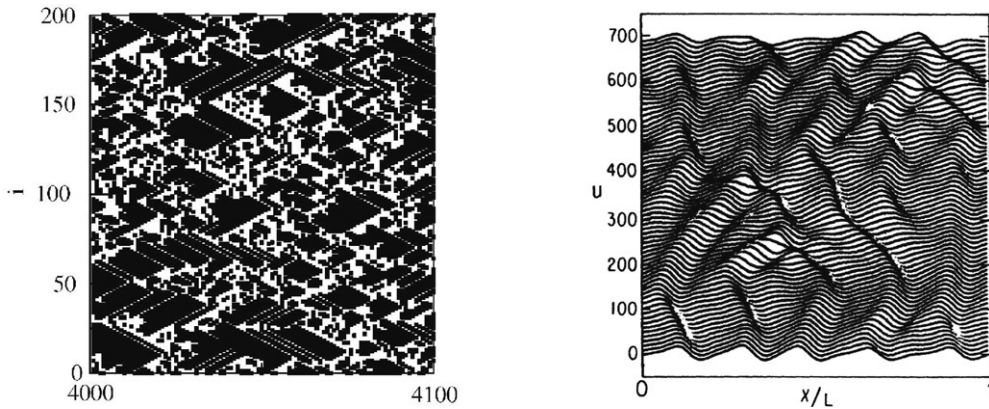


Fig. 1a. Left: space–time diagram of a CML. Black (white) dots correspond to sites in a laminar (chaotic) regime. Horizontal (vertical) axis represents time (space). From [111]. Right: space–time diagram of a solution of the KS equation (2). The distribution of the field variable $u(x)$ is plotted in a sequence of snapshots. Reprinted with permission from [37].

© 1986, by the American Physical Society, see <http://link.aps.org/abstract/PRL/v57/p325>.

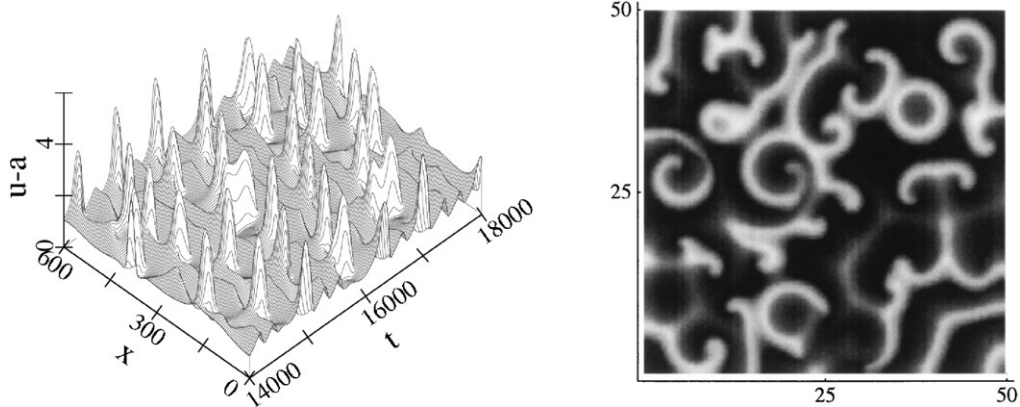


Fig. 1b. Left: space–time diagram of an RD problem in one spatial dimension. The third axis represents the difference between the two concentrations. From [35]. Right: instantaneous spatial pattern of an excitable medium in two dimensions. Shading corresponds to the concentration of one substance. The pattern is similar to that of a cGL equation. Reprinted with permission from [49].

© 1998, by the American Physical Society, see <http://link.aps.org/abstract/PRL/v80/p2306>.

A convenient way of representing an infinite dimensional phase space is to expand the field variable(s) in terms of a complete set of orthonormal basis functions. The expansion coefficients a_i , $i = 1, \dots$ can also be considered as phase–space variables. This expansion can be truncated at some index N if variables a_i with $i = N + 1, N + 2, \dots$ are negligible from the point of view of global dynamics. Thus, even systems described by partial differential equations can be represented as high-dimensional systems with a finite number $N \gg 1$ of degrees of freedom.

Stationary solutions do not depend on time, and correspond thus to fixed points of the phase space. Stable stationary solutions appear as fixed-point attractors. Homogeneous periodic solutions or waves correspond to limit cycles. Complicated chaotic solutions can be associated with other parts of the phase space, in the form of either chaotic attractors or chaotic saddles. The phenomenon of long transients is most naturally related to situations where the chaotic set is a saddle and, in addition, this saddle is rather dense (although not entirely space filling).

2.3. Spatiotemporal intermittency

There is substantial literature on the so-called spatiotemporal intermittency (STI) [10–14,1,5]. Here we briefly review this phenomenon, in order to distinguish it from concepts appearing later in this paper. In dynamical systems theory, intermittency denotes irregular alternations between temporally simple and irregular phases. The concept of

STI applies to spatiotemporal systems in which any spacetime point can be classified as either *laminar* or *turbulent*. By “laminar” we mean a regular pattern (whose temporal dynamics might be both regular and chaotic), while “turbulent” regions have no apparent regularity either in space or in time. Spatiotemporal intermittency implies that there are intervals in both space and time in which one of the phases dominates. Domains of a given type of behavior have well-defined boundaries. An example is provided by the left panel of Fig. 1a. By now there is a long list of experiments on STI in several different problems (for a few recent examples see [15–17]).

Spatiotemporal intermittency is not the only possible, but certainly a typical appearance of spatiotemporal chaos. It can be considered as a transition between ordered patterns and fully developed spatiotemporal chaos (between fully laminar and fully turbulent phases). This does not imply that STI must evolve to be more and more complicated. Spatiotemporal intermittency can very well provide an asymptotic state, a spatiotemporally chaotic attractor.

The usual statistical measures of STI consider long time averages of spatial characteristics, such as the distribution of the size of laminar regions and that of the “turbulent” regions [12,13]. In a spatiotemporally intermittent state both distributions are exponentially decaying. The decay constants are related to the sizes of the average laminar or turbulent phases. A difference between the character of these distributions shows up at the onset of STI. Here the distribution of the laminar domains follows a power law, indicating the lack of any characteristic sizes. The onset is, therefore, similar to a phase transition.

In fact, two different types of STI can be distinguished [1,5]. In the first type of STI, discovered by Kaneko [10] and Chaté and Manneville [12,13], the laminar state is spatially homogeneous, and there is no spontaneous creation of turbulent bursts if a site and its neighbors are laminar. The mentioned analogy with phase transitions is then complete, and the transition belongs to the universality class of directed percolation [13,18]. In the second type of STI, first described by Keeler and Farmer [11] and Kaneko [14], there is some spatial structure present before the onset of STI, and turbulent bursts might be created even if a site and its neighbors are laminar. This STI is more robust than the first one. There is, however, no universal behavior below the critical point, and even at the critical point scaling might set in very late. The spontaneous generation of turbulent bursts has been conjectured [5] to be related to dynamical phenomena like riddled basins and on–off intermittency [19,20].

We wish to emphasize that STI can also characterize long transients [14,21,22]. In fact, many of the transients in spatiotemporal systems are of this type. We shall see that the lifetime can be sufficiently long to make statistical properties stationary (similar to, e.g. the statistics needed to determine the average Lyapunov exponent on a chaotic saddle in low-dimensional systems).

3. Supertransients in low-dimensional dynamical systems

Transient chaos encountered in low-dimensional systems is usually not supertransient in the sense that its average lifetime τ obeys the familiar algebraic scaling law with parameter variation [23,24]:

$$\tau(p) \sim (p - p_c)^{-\alpha}, \quad p > p_c, \quad (8)$$

where p is a system parameter, p_c is a critical value, and $\alpha > 0$ is the algebraic scaling exponent. Supertransients (in low-dimensional systems also called *superpersistent chaotic transients*) are characterized by the following scaling law for their average lifetime [8,25]:

$$\tau(p) \sim \exp[C(p - p_c)^{-\chi}], \quad (9)$$

where $C > 0$ and $\chi > 0$ are constants. As p approaches the critical value p_c from above, the transient lifetime τ becomes superpersistent in the sense that the exponent in the exponential dependence diverges. This type of chaotic transients was conceived to occur through the dynamical mechanism of unstable–unstable pair bifurcation, in which an unstable periodic orbit in a chaotic attractor collides with another unstable periodic orbit pre-existed outside the set [8,25]. The same mechanism was believed to cause riddling bifurcation [20] that creates a riddled basin [19], so supertransients can be expected at the onset of riddling.

3.1. Unstable–unstable pair bifurcation and scaling of average transient lifetime

Unstable–unstable pair bifurcation represents a generic mechanism for superpersistent chaotic transients [8,25,20]. One can imagine two unstable periodic orbits of the same period, one in a chaotic attractor and another on the basin

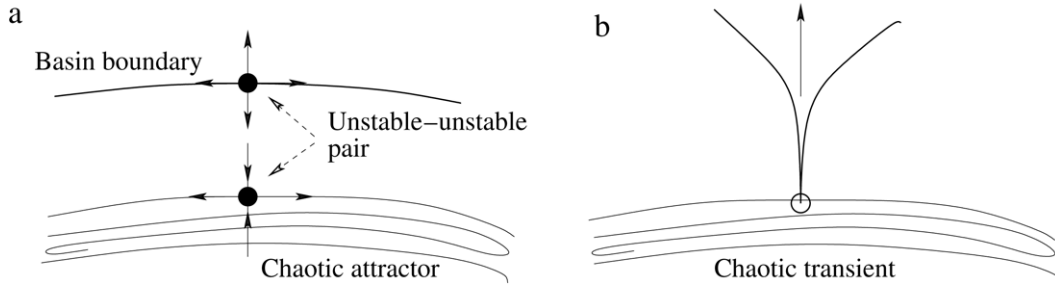


Fig. 2. Unstable–unstable pair bifurcation. (a) Invariant sets for $p < p_c$: a chaotic attractor, the basin boundary, and the pair of unstable periodic orbits. (b) For $p > p_c$, an escaping channel is created by an unstable–unstable pair bifurcation that converts the originally attracting motion into a chaotic transient.

boundary, as shown in Fig. 2(a). As a bifurcation parameter p reaches a critical value p_c , the two orbits *coalesce* and disappear simultaneously, leaving behind a “channel” in the phase space through which trajectories on the chaotic attractor can escape, as shown in Fig. 2(b). The chaotic attractor is thus converted into a chaotic transient, but the channel created by this mechanism is typically supernarrow [8,25,20]. Suppose on average, it takes time $T(p)$ for a trajectory to travel through the channel in the phase space so that it is no longer on the attractor. We expect the tunneling time $T(p)$ to be infinite for $p = p_c$ but, for $p > p_c$ the time becomes finite and decreases as p is increased from p_c . For p above but close to p_c , the tunneling time can be long.

From Fig. 2(a), we see that if the phase–space is two dimensional, the periodic orbit on the attractor must be a saddle and the one on the basin boundary must be a repeller. This can arise if the map is noninvertible. Thus, the unstable–unstable pair bifurcation can occur in noninvertible maps of at least dimension two, or in invertible maps of at least dimension three (or in flows of dimension of at least four).

Let $\lambda > 0$ be the largest Lyapunov exponent of the chaotic attractor. After an unstable–unstable pair bifurcation the opened channel is locally transverse to the attractor. A trajectory which spends time $T(p)$ in the channel centered about an earlier existing unstable periodic orbit on the attractor must come to within a distance of about $\exp[-\lambda T(p)]$ from this orbit. The probability for this to occur is proportional to $\exp[-\lambda T(p)]$. The average time for the trajectory to remain on the earlier attractor, or the average transient lifetime, is thus related to the tunneling time as

$$\tau(p) \sim \exp[\lambda T(p)]. \tag{10}$$

To obtain the scaling dependence of the tunneling time $T(p)$ on $p - p_c$, we note that, since the escaping channel is extremely narrow, for typical situations the dynamics in the channel is approximately one dimensional [Fig. 2]. The basic dynamics can be captured through the following simple one-dimensional map:

$$x_{n+1} = x_n^{k-1} + x_n + p, \tag{11}$$

where x denotes the dynamical variable in the channel, $k \geq 3$ is an odd integer to generate two real fixed points, and p is a bifurcation parameter with critical point $p_c = 0$. For $p < p_c = 0$, the map has a stable fixed point $x_s = -|p|^{1/(k-1)}$ and an unstable fixed point $x_u = |p|^{1/(k-1)}$. These two collide at p_c and disappear for $p > p_c$, mimicking an unstable–unstable pair bifurcation.

Since for $0 < p \ll 1$, $T(p)$ is large, map (11) can be approximated in continuous time by the differential equation:

$$\frac{dx}{dt} = x^{k-1} + p. \tag{12}$$

Suppose the root of the channel is $x = 0$ and its length is l . The tunneling time is then

$$T(p) \approx \int_0^l \frac{dx}{x^{k-1} + p} \sim p^{-\frac{k-2}{k-1}}. \tag{13}$$

Substituting Eq. (13) into Eq. (10) gives

$$\tau(p) \sim \exp(Cp^{-\frac{k-2}{k-1}}), \tag{14}$$

where $C > 0$ is a constant. We see that as p approaches the critical value $p_c = 0$ from above, the average transient lifetime diverges in an exponential-algebraic way, giving rise to supertransients. Exponent χ of relation (9) assumes thus the value of $(k - 2)/(k - 1) < 1$.

3.2. A classical example

A classical two-dimensional model system exhibiting supertransients is the one considered by Grebogi, Ott, and Yorke [8,25], as follows:

$$\theta_{n+1} = 2\theta_n \bmod 2\pi, \quad z_{n+1} = az_n + z_n^2 + \beta \cos \theta_n, \quad (15)$$

where a and β are parameters. Because of the z_n^2 term in the z -equation, for large z_n we have $|z_{n+1}| > |z_n|$. There is thus an attractor at $z = +\infty$. Near $z = 0$, depending on the choice of the parameters, there can be either a chaotic attractor or none. For instance, for $0 < \beta \ll 1$, there is a chaotic attractor near $z = 0$ for $a < a_c = 1 - 2\sqrt{\beta}$ and the attractor becomes a chaotic transient for $a > a_c$ [8]. The chaotic attractor, its basin of attraction, and part of the basin of the infinity attractor are shown in Fig. 3.

Following the same argument leading to the scaling law (14), one can see that map (15) allows for a supertransient for $a > a_c$. In particular, for $a < a_c$ there are two fixed points: $(0, z_+)$ and $(0, z_-)$, where $z_{\pm} = (1 - a \pm \sqrt{(1 - a)^2 - 4\beta})/2$ on the basin boundary and on the chaotic attractor, respectively. They coalesce at $a = a_c$. For $a > a_c$, a channel is created through which trajectories on the original attractor can escape to an attractor at infinity. At the location of the channel where $\theta = 0$, the z -mapping reads as $z_{n+1} = az_n + z_n^2 + \beta$. Letting $\delta = z - z_*$, where $z_* = (1 - a)/2$, we obtain

$$\delta_{n+1} = \delta_n^2 + \delta_n + b, \quad (16)$$

with $b = \sqrt{\beta}(a - a_c) - [(a - a_c)/2]^2$. For $a \approx a_c$, we have $b \approx \sqrt{\beta}(a - a_c)$. Eq. (16) is identical to Eq. (11) with $k = 3$. Integral (13) then yields $T \approx \pi b^{-1/2}/2$. Since the Lyapunov exponent is determined by the θ -dynamics, $\lambda = \ln 2$, and in view of (10), the average chaotic transient time is given for $a > a_c$ by

$$\tau(a) \sim e^{T \ln 2} \approx e^{(\pi \ln 2/2)b^{-1/2}} \approx e^{C(a - a_c)^{-1/2}}, \quad (17)$$

where $C = \pi(\ln 2)\beta^{-1/4}/2$ is a positive constant.

4. Supertransients in spatially extended dynamical systems

4.1. Transient chaos in coupled map lattices

Perhaps the first indication of complex spatiotemporal patterns appearing as long lived transients was found in the thermal convection experiments by Ahlers and Walden, as early as 1980 [26]. For a detailed investigation of these transients, however, CMLs have proven to be the most appropriate model systems, initiated by the seminal paper of Crutchfield and Kaneko [27].

The CML (1) has been studied extensively for different types of maps f . The initial conditions are most frequently taken as random numbers at each site. When the map is strictly contracting, the asymptotic behavior is always a spatially regular and temporally periodic (often homogeneous and steady) behavior. The transients towards this state are, however, typically chaotic. For maps f that produce transient chaos on their own with positive topological entropy but possess periodic attractors, the asymptotic behavior is most often again spatially regular and temporally periodic. The CML built on map f with chaotic attractors generates permanent spatiotemporal chaos if the coupling is weak, but transient chaos leading to a simple attractor seems to be the common behavior for intermediate and strong couplings [22]. These typical findings are summarized in Table 1. We can thus say that diffusive coupling appears to generate topological chaos even from nonchaotic maps, and often converts permanent local chaos into global transients.

An interesting question is how the average lifetime, τ , of transients towards a simple attractor depends on the system size, L . At weak coupling, $\varepsilon < \varepsilon_0$, practically no size dependence is found. At stronger (but yet weak) coupling,

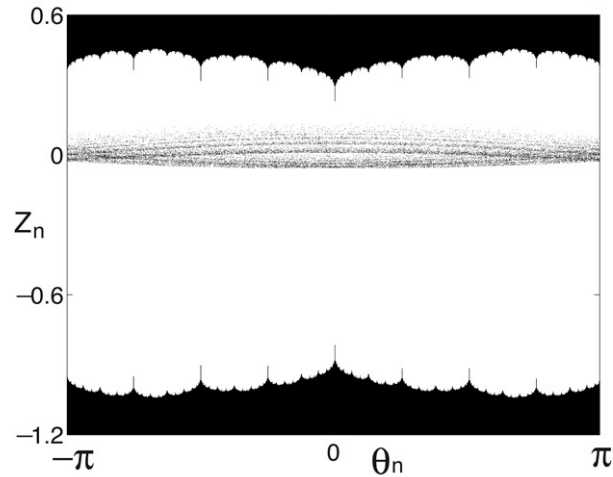


Fig. 3. Phase space of the two-dimensional map model (15): a chaotic attractor near $z = 0$ (black), its basin of attraction (blank), and the basin of attraction of the attractor at $z = +\infty$ (black) for $a = 0.5$ and $\beta = 0.04$.

Table 1
Dynamics of map f and of the corresponding CML

Map f	CML
Non-chaotic	Transiently chaotic [27–31,9]
Transiently chaotic	Transiently chaotic [32]
Permanently chaotic	Transiently chaotic [21,22,33] Permanently chaotic [34,21,22]

however, the lifetime increases rapidly with the system size. This is the class called supertransient by Crutchfield and Kaneko [27]. Two basically different types can be distinguished:

Type-I supertransients are characterized by a power-law scaling

$$\tau(L) \sim L^\sigma \tag{18}$$

with a positive exponent σ .

Type-II supertransients are characterized by an exponential scaling:

$$\tau(L) \sim \exp(aL^\gamma). \tag{19}$$

Here γ is a positive exponent, and the coefficient a may depend on the system parameters.

The appearance of the patterns related to these types of supertransients is qualitatively different. In particular, for Type-I supertransients, the basic features are defects whose density decreases gradually with time, as shown in Fig. 4. This can also be considered as a kind of aging process. Correspondingly, dynamical invariants such as the Lyapunov exponents and entropies also decrease with time.

Type-II supertransients are, in contrast, statistically steady over a long period of time, i.e., averages are time-independent in the chaotic state, and the transition to an attractor is rather abrupt (see Fig. 5). If the maximum Lyapunov exponent is positive in the chaotic state, a chaotic saddle is expected to exist in the high-dimensional phase space. The Lyapunov exponents of the chaotic saddle provide the time-independent exponents for the transients.

4.2. The origin of supertransient scaling

The different scaling rules can be traced back to the different patterns characteristic of the two main subclasses of supertransients.

Type-I supertransients: The dominant process is that the defects, as indicated by Fig. 4, undergo a kind of random walk and when they meet, they annihilate. For an anomalous random walk the variance of the displacement scales

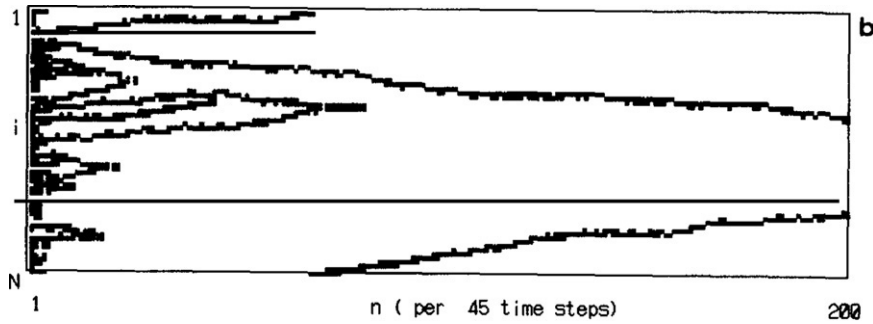


Fig. 4. Typical space-time pattern of Type-I supertransients. From [32].

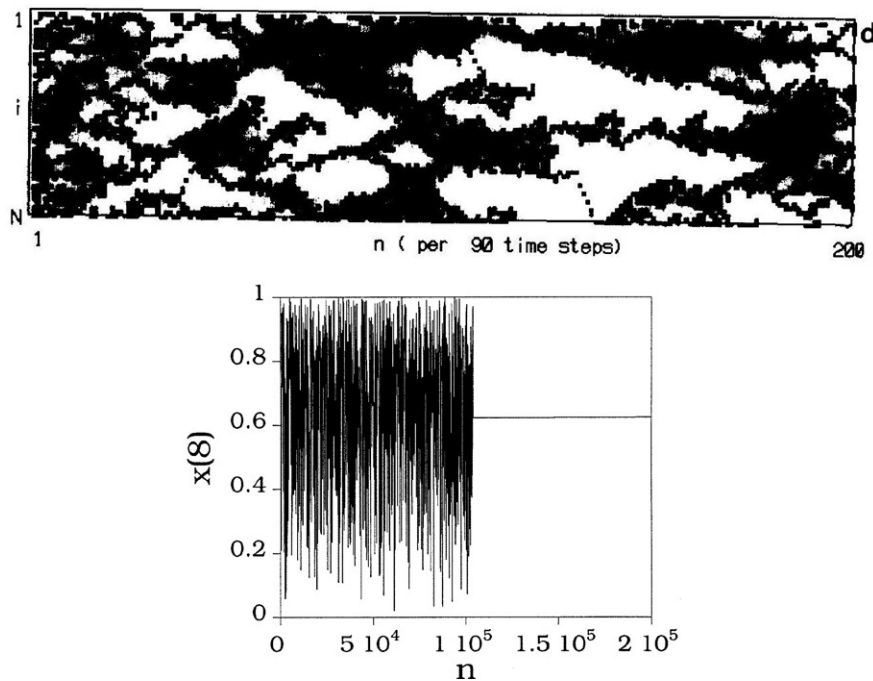


Fig. 5. Top panel: Typical space-time pattern of Type-II supertransients. From [32]. Bottom panel: Time dependence at a single site illustrates that the crossover to the nonchaotic behavior is abrupt. Reprinted with permission from [33]. © 1995, by the American Physical Society, see <http://link.aps.org/abstract/PRL/v74/p5208>.

with time as $t^{1/\sigma}$ where σ is a positive parameter ($\sigma = 2$ corresponds to normal diffusion). Estimating the average lifetime τ as the time needed to reach a displacement variance of the order of the system size, we obtain $\tau \sim L^\sigma$, which is (18).

Type-II supertransients: Let $x^*(i)$ denote the coordinate corresponding to the regular spatiotemporal attractor at site i [$x^*(i)$ might also be time-periodic]. One can find a basin size r , much smaller than the system size in the following sense: if $|x_0(i) - x^*(i)| < r$ for *all* sites, the system reaches the attractor without chaotic excursions, but if the difference is larger than r , irregular transients appear. This basin size is a measure of the extension of the attractor’s basin, restricted to a single dimension. The probability P that a randomly chosen initial condition at some of the sites falls within the basin size is proportional to this size: $P \sim r \ll 1$.

The following intuitive argument has been applied by different authors [32,29,21,35] to explain the scaling with the system size. In spatially extended systems there always exists a correlation length ξ within which neighboring sites move in a coherent manner. Conversely, only sites further away from each other than ξ move independently. The system can thus be divided in L/ξ subunits which behave independently. For a random initial condition of the full CML, the probability Π to fall into all the local basins is P raised to the number of independent units, i.e., $\Pi \sim P^{L/\xi}$.

Time needed to reach the hole of the phase space corresponding to the basin size is proportional to $1/\Pi$, thus the average lifetime is estimated as

$$\tau(L) \sim \Pi^{-1} \sim P^{-L/\xi} \sim e^{aL} \quad (20)$$

where $a = (\ln 1/P)/\xi$ is a positive constant. Here we have assumed that the basin size is independent of the system size. A strong L dependence of r can modify the result. If, for example, $r = r(L) \sim \exp(-L^\nu)$, we find $\tau(L) \sim \exp(L^\nu/\xi)$ [cf. (19)]. The majority of numerical findings supports, however, a linear length dependence in the exponent, and therefore an at most weakly L -dependent basin size.

Finally we note that the problem of supertransients might be considered as the high-dimensional analog of the chaoticity of well stirred chemical reactions in *closed* containers. In the lack of any material flux, the final state can only be in thermal equilibrium, governed by a fixed-point attractor. With initial conditions far away from the thermal equilibrium, one brings the system into a nonlinear regime and long chaotic transients appear, as pointed out by Scott, Showalter and coworkers [36]. The novel feature in spatiotemporal cases is that nearly all initial conditions are automatically far away from the attractor since the basin of attraction is extremely small.

4.3. Supertransients with exponentially long lifetimes in other systems

It is remarkable that supertransients, mainly of Type-II, appear in a plethora of systems more complicated than CMLs. Typically, the lifetime scales as a simple exponential of the system size:

$$\tau(L) \sim \exp(aL). \quad (21)$$

Evidence for this behavior has been found in a number of systems, as follows.

Kuramoto–Shivashinsky equation: The investigations of Shraiman [37] and of Hyman, Nicolaenko and Zalesky [38] of phase turbulence in the one-dimensional KS equation (2) provided the first examples of supertransients in a PDE system, discovered earlier than those in CMLs. The right panel of Fig. 1a shows a typical transient pattern.

Complex Ginzburg–Landau equation: After a detailed numerical analysis of long lasting spatiotemporal turbulence in the two-dimensional cGL equation by Bohr and coworkers ([39,40,3]), Braun and Feudel [41] provided numerical evidence for an exponential scaling with the system size.

Reaction–diffusion systems: The first clear example of Type-II supertransients in RD systems of the type (5) in one spatial dimension was found by Wacker, Bose and Schöll [35]. A typical concentration distribution in the transient phase can be seen in the left panel of Fig. 1b. A decomposition of patterns during the transients into eigenmodes indicates that there exist no preferred modes [42–44]. Transient patterns are thus shown to be uncorrelated, a feature underlying the argument of the previous section leading to Type-II supertransient scaling. The study of RD systems has recently been extended by Wackerbauer, Showalter and coworkers [45–48].

Two-dimensional excitable medium: The model investigated by Strain and Greenside [49] differs slightly in structure from (5), but exhibits similar dynamical behavior, although with different types of patterns in two dimensions (see right panel of Fig. 1b). This is the first PDE model in which fractal properties of a high-dimensional chaotic saddle have been investigated (see Section 7).

Complex networks: A surprising recent observation of Zumdieck, Timme, Geisel, and Wolf [50] is that in a randomly diluted set of coupled oscillators the transients towards a limit cycle attractor are chaotic and exhibit scaling (21) with the number of oscillators replacing the length L . The average lifetime of transients depends also on the network connectivity, and reaches a maximum at intermediate dilution. Irregular and exponentially long transients are also observed in a diluted neural network model [51].

Turbulent shear flow: Theoretical work of Eckhardt and coworkers (see, e.g., [52,53]) based on the Navier–Stokes equation (6) has predicted the long-lived transient nature of turbulence in pipes. A recent experiment by Hof et al. [54] provides evidence for a Type-II supertransient scaling, where variable L in (21) is replaced by the Reynolds number (7) (for more detail see Section 8).

4.4. Stable chaos

A peculiar feature of Type-II supertransients is that the maximum Lyapunov exponent is in certain cases negative even *during the transients*, although the transient patterns are as irregular as otherwise. This phenomenon has been

called stable chaos [9,31] and provides an example where linear stability can coexist with nonlinear instability in the transient phase.

Following a definition of Politi and coworkers [51], stable chaos means transients characterized by (i) a negative or zero maximum Lyapunov exponent, (ii) appearing to be stationary for long times (iii) which scales exponentially with the system size. The phenomenon is robust also in the sense that it can be present in finite regions of the parameter space [9].

Stable chaos has first been found in CML-s where the local map f is piecewise linear, discontinuous in certain points, and possesses a simple periodic attractor. Map f might be contracting [27,29], or might also have expanding pieces [9,55,56]. The transients are in any case random, illustrated by an exponential decay of both temporal and spatial correlations. One might think that these features are due to the artificial discontinuity of f , but a continuous variant of the map, where the jump is replaced by a very steep continuous line, has been shown to provide the same behavior [29,9]. The supertransients with such discontinuous maps, or with their nearby continuous variants, appear to be nonchaotic in the sense of sensitive dependence to initial conditions, but are chaotic in the sense of topological complexity. The irregular behavior of stable chaos cannot be related to a local production of information due to the lack of a positive Lyapunov exponent. A careful investigation [31,57–59] leads to the conclusion that irregularity of stable chaos is produced by transport, by the nonlinear propagation of finite disturbances from the outer regions, or the boundaries, of the chain. This is in analogy with what one knows for chaotic CA rules, and therefore the so-called *damage spreading* analysis [2] can successfully be applied. One is interested then in the effect produced by finite localized perturbations. Indeed, in systems exhibiting stable chaos [31,57–59] initially perturbed regions in space spread with a *constant* front velocity, v . Disturbances can thus travel undamped through the system, and it is this velocity which plays in some sense the role of a positive Lyapunov exponent.

Stable chaos often appears in a certain range of a control parameter, e.g., of the coupling constant ε in (1). Outside this range, there are no long transients, the system rapidly reaches the synchronized, periodic state, where the front velocity v is zero. The transition is, however, not a single point in the parameter space. It occurs in an extended interval, a ‘fuzzy region’ [58], where ordered and chaotic dynamics characterized by $v = 0$ and $v \neq 0$, respectively, alternate in a quite irregular manner.

The fact that stable chaos is not restricted to CML-s has also been demonstrated. Bonaccini and Politi [60] have considered coupled nonchaotic oscillators in continuous time. The oscillators are subjected to a synchronous periodic forcing over a period T , which is suddenly changed to an unforced state of length T' , and this mechanism is repeated periodically. For sufficiently rare active driving, T/T' small, the largest Lyapunov exponent of the coupled-driven system is negative, and the system exhibits properties of stable chaos. In a completely different context, stable chaos has been found in a one-dimensional model of heat conductivity based on a diatomic gas of hard-point particles [61,62]. In these examples, direct numerical evidence for an exponential scaling of the transient lifetime has not been given, although this is very plausible on general grounds. The diluted neural network model [51] mentioned in Section 4.3 is shown to follow (21) in a certain range of parameters, and is also characterized by negative Lyapunov exponents, during the transients.

In all the examples, the dynamics is associated with the presence of discontinuities, or with being close to such singularities. In the oscillator model there is a sudden change in the driving mechanism; in the hard point gas discontinuity arises in connection with three-body collisions where ordering changes abruptly, and in the neural model the discontinuity is connected with changes in the spike ordering. Thus one can conclude [51,62] that it is the presence of discontinuities in the phase space which appears to be a necessary condition for the onset of stable chaos.

5. Effect of noise on supertransients

5.1. Low-dimensional systems

In the general setting where an unstable–unstable pair bifurcation can occur (see Section 3), noise can induce supertransients preceding the bifurcation. Consider, in the noiseless case, a chaotic attractor in its basin of attraction ($p < p_c$). When noise is present, there can be a nonzero probability that two periodic orbits, one belonging to the attractor and another to the basin boundary, can get close and coalesce *temporally*, giving rise to a nonzero probability that a trajectory on the chaotic attractor crosses the basin boundary and moves toward the basin of another attractor. Transient chaos thus arises even for $p < p_c$. Due to noise, the channels through which trajectories escape the chaotic

attractor open and close intermittently in time. Escaping through the channel requires staying of the trajectory in a small vicinity of the opening of the channel for a finite amount of time, which is an event with extremely small probability. For a two-dimensional phase space, the situation described above can be schematically illustrated as in Fig. 2(a) and (b), respectively, for the cases where noise is absent and present. As for Eq. (10), the average lifetime of noise-induced supertransient can be expressed in terms of the tunneling time $T(p, \sigma)$ as

$$\tau(p, \sigma) \sim \exp[\lambda T(p, \sigma)], \tag{22}$$

where $\lambda > 0$ is (as in Section 3) the largest Lyapunov exponent of the original chaotic attractor. We note that, since the escaping channel is extremely narrow, for $T(p, \sigma)$ large, the dynamics in the channel is approximately one dimensional along which the periodic orbit on the attractor is stable but the orbit on the basin boundary is unstable for $p < p_c$ [Fig. 2(a)]. This feature can thus be captured through the stochastic version of map (11):

$$x_{n+1} = x_n^{k-1} + x_n + p + \sigma \xi(n), \tag{23}$$

where σ is the noise amplitude, and $\xi(n)$ is a Gaussian random variable of zero mean and unit variance. For $T \gg 1$, Eq. (23) can be approximated by the Langevin equation

$$\frac{dx}{dt} = x^{k-1} + p + \sigma \xi(t). \tag{24}$$

For $p < 0$, the deterministic system for Eq. (24) has a stable and an unstable fixed point but there are no more fixed points for $p > 0$, as shown in Fig. 6. Let $P(x, t)$ be a probability density function of the stochastic process governed by Eq. (24). This density function satisfies the Fokker–Planck equation [63,64]:

$$\frac{\partial P(x, t)}{\partial t} = -\frac{\partial}{\partial x}[(x^{k-1} + p)P(x, t)] + \frac{\sigma^2}{2} \frac{\partial^2 P}{\partial x^2}. \tag{25}$$

Let l be the effective length of the channel in the sense that a trajectory with $x > l$ is considered to have escaped the channel. The tunneling time $T(p, \sigma)$ required for a trajectory to travel through the channel is equivalent to the mean first passage time from the opening, x_r , of the channel to l . Our interest is in the trajectories that do escape. For such a trajectory, we assume that once it falls into the channel through x_r , it will eventually exit the channel at $x = l$ without even going back to the original chaotic attractor. This is reasonable considering that the probability for a trajectory to fall in the channel and then to escape is already exponentially small [Eq. (22)] and, hence, the probability for any “second-order” process to occur, where a trajectory falls in the channel, moves back to the original attractor, and falls back in the channel again, is negligible. For trajectories in the channel there is thus a reflecting boundary condition at $x = x_r$:

$$\left[(x^{k-1} + p)P(x, t) - \frac{\sigma}{2} \frac{\partial P}{\partial x} \right] \Big|_{x=x_r} = 0. \tag{26}$$

That trajectories exit the channel at $x = l$ indicates an absorbing boundary condition at $x = l$:

$$P(l, t) = 0. \tag{27}$$

Assuming that trajectories initially are near the opening of the channel (but in the channel), we have the initial condition

$$P(x, x_r) = \delta(x - x_r^+). \tag{28}$$

Under these boundary and initial conditions, the solution to the Fokker–Planck equation yields the following mean first-passage-time [63,64] for the stochastic process (24):

$$T(p, \sigma) = \frac{2}{\sigma^2} \int_{x_r}^l dy \exp \left[-\frac{H(y)}{\sigma^2} \right] \int_{x_r}^y \exp \left[\frac{H(y')}{\sigma^2} \right] dy' \tag{29}$$

where

$$H(x) = (x^k/k + px)$$

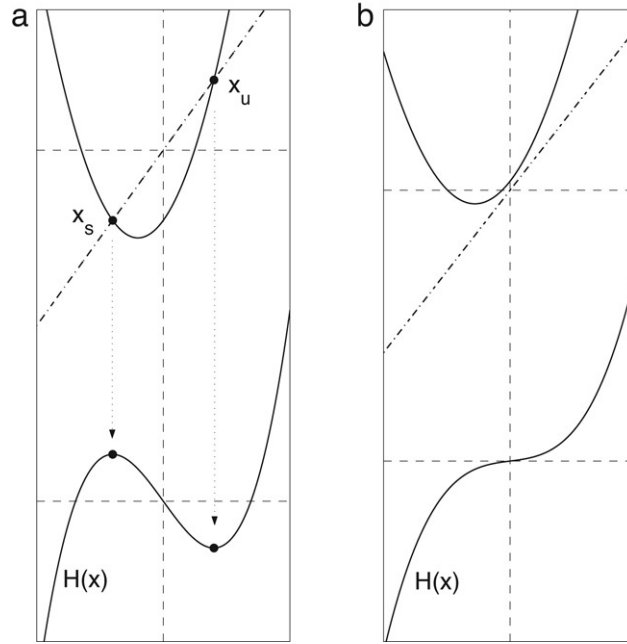


Fig. 6. Dynamics of map (23), for $k = 3$ (a) in the subcritical cases ($p < 0$), and (b) in the supercritical case ($p > 0$). Upper graph: deterministic map ($\sigma = 0$), lower graph: stochastic potential $H(x)$ (cf. text).

is a so-called stochastic potential. In the most interesting weak noise regime ($\sigma \ll \sigma_c \sim |p|^{k/(2(k-1))}$), the results can be summarized as follows,

$$T(p, \sigma) \sim \begin{cases} p^{-(k-2)/(k-1)}, & p > 0, \\ \sigma^{-(2-4/k)}, & p = 0, \\ |p|^{-(k-2)/(k-1)} \exp(|p|^{k/(k-1)}/\sigma^2), & p < 0. \end{cases} \quad (30)$$

These laws imply the following scaling laws for the average lifetime of the chaotic transients in various regimes [substituting the expressions of $T(p, \sigma)$ in Eq. (22)]:

$$\tau(p, \sigma) \sim \begin{cases} \exp[Cp^{-(k-2)/(k-1)}], & p > 0, \\ \exp[C\sigma^{-(2-4/k)}], & p = 0, \\ \exp\left(C|p|^{-(k-2)/(k-1)} \exp[|p|^{k/(k-1)}/\sigma^2]\right), & p < 0. \end{cases} \quad (31)$$

The general observation is that three behaviors arise in the noise dependence of τ depending on the bifurcation parameter p : independent of noise for the supercritical regime [the same as in the deterministic case (cf. (14))], normally superpersistent for the critical case, and extraordinarily superpersistent for the subcritical regime in the sense of scaling in (31) (for $p < 0$). Numerical support for these distinct scaling behaviors have been obtained [65, 66].

Noise-induced supertransients were demonstrated [67] in phase synchronization [68] of weakly coupled chaotic oscillators. Signatures of noise-induced supertransients were also found [69] in the advective dynamics of inertial particles in open fluid flows [70].

5.2. Effect of noise and nonlocal coupling on supertransients in spatially extended dynamical systems

The first numerical effort to clarify the effect of noise on supertransients in spatially extended dynamical systems was published in Ref. [71], where a CML system was investigated. The diffusive coupling constant ε in (1) was replaced by a random variable $\varepsilon \rightarrow \varepsilon + \sigma \xi_n$ where ξ_n is a random number taken at time instant n , and σ represents the noise intensity, assumed to be small. This choice of noise is homogeneous over the full system, i.e., ξ_n does not

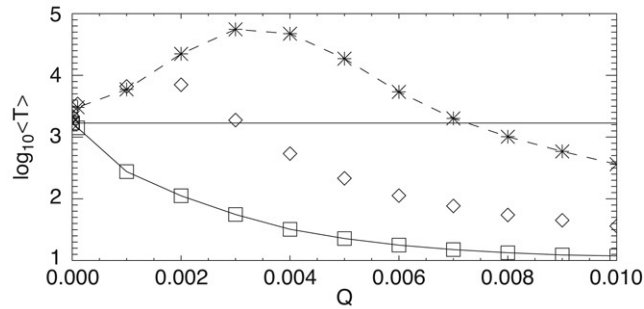


Fig. 7. Dependence of the average lifetime $\langle T \rangle \equiv \tau$ on the noise intensity $Q \equiv \sigma$ in an RD system. The degree of spatial noise inhomogeneity r decreases from $r = 20$ (stars) to $r = 4$ (diamonds) to spatially homogeneous noise $r = 1$ (squares). Reprinted with permission from [47].

© 2007, by the American Physical Society, see <http://link.aps.org/abstract/PRE/v75/p066209>.

depend on the site index i . The average lifetime was found to hardly depend on the noise intensity σ in the interesting regime of weak noise. This supports the view that supertransients are robust.

A more recent investigation of Wackerbauer and Kobayashi [47] considered the effect of spatially inhomogeneous noise as well. They have studied an RD system [Eq. (5)] in one spatial dimension with periodic boundary condition. The continuous space dependence in the concentrations $a(x, t)$, $b(x, t)$ is approximated by a discrete set $a^{(i)}(t)$, $b^{(i)}(t)$ of variables at $N \gg 1$ sites ($i = 1, \dots, N$). Correspondingly, the diffusive coupling is also discretized. This chain of variables can be considered to be arranged around a circle. Additive noise $\sigma \xi^{(i)}(t)$ is included in the chemical kinetic equation of the concentration $b^{(i)}$. The chain is divided into r blocks such that N/r neighboring sites are subject to the same realization of noise. The noise terms acting on neighboring blocks are chosen to be independent. Any value $r > 1$ corresponds to a spatially inhomogeneous noise, the more inhomogeneous the larger r . The results show that spatially inhomogeneous noise tends to increase the lifetime of supertransients for weak noise up to a certain strength where a maximum is reached, as seen in Fig. 7. The effect intensifies with the degree of inhomogeneity parameter r . The scenario is similar to what occurs in a class of low-dimensional systems [72,73]. Qualitatively, a weak inhomogeneous noise makes the system more random and reduces the chance to find the small basin around the attractor. Interestingly, homogeneous noise ($r = 1$) has in this model a destructive effect on the transients: it produces a monotonous decrease of the lifetime for increasing noise strength. It is important to mention that irrespective of the kind of change induced by noise, i.e., even if the average lifetime was drastically decreased, the Type-II supertransient scaling remains valid: lifetime increases exponentially with the size for any fixed type of noise. The strength of increase changes slightly: coefficient a in (21) becomes weakly dependent on noise intensity: $a \rightarrow a(\sigma)$ so that $a(\sigma) > a(0)$ when the average lifetime is larger than that without noise, and vice versa.

In search for a control of the length of supertransients, an approach is to investigate the effect of nonlocal coupling in the noise-free problem. In the aforementioned model Yonker and Wackerbauer [46] studied the consequence of adding a few nonlocal connections (shortcuts). At sites coupled not only to the next neighbors but to a third, further site, they modified the discrete Laplacian so that all three sites are included in a way that ensures the same perturbation, the same as in the locally coupled model. The length s of the shortcuts turns out to be a basic parameter. It is defined as the minimal number of sites between the two end sites of the shortcut, divided by the number N of sites in the ring. The longest shortcut connecting two opposite sites along the circle corresponds to length $s = 1/2$. For a single shortcut of small length, the average lifetime increases, reaches a maximum about $s = 0.05$, then decreases, finally leading to a reduced lifetime compared to that in the locally coupled system. The overall dependence is similar to that of the upper curves in Fig. 7. It is important again that the Type-II supertransient scaling remains valid for any s with a slightly s -dependent prefactor $a(s)$ in (21).

Adding more shortcuts can have a drastic effect on the transients. For example, two will have a local effect which can stabilize spatiotemporal chaos for arbitrarily long times, effectively preventing its collapse. Whether this can actually happen depends on the locations of the shortcuts and the initial conditions. For example, in a large ensemble of cases with randomly chosen shortcut locations, in about 70% of the cases, spatiotemporal chaos appears to be permanent. Three shortcuts can increase the likelihood of permanent chaos even more. A further increase of the number of shortcuts, however, seems to weaken the effect, and the likelihood of transient chaos increases again.

Control of spatiotemporal transients via nonlinear feedbacks was first suggested by Qu and Hu [21]. They considered a CML and demonstrated that proper control can shorten the lifetime of the transients by several orders of magnitude. These developments illustrate that adding weak noise, or taking over methods from the physics of networks, might provide some effective ways to harness transient chaos in spatially extended systems.

6. Crises in spatiotemporal dynamical systems

6.1. Supertransients preceding asymptotic spatiotemporal chaos

When there is an asymptotic spatiotemporal chaotic attractor, or asymptotic “turbulence,” long chaotic transients typically occur in a parameter range preceding the permanently chaotic regime. Suppose the latter is in the parameter range $p > p_1$. Chaotic transients are then present for $p < p_1$. It can be seen intuitively that their average length should increase upon approaching the critical value p_1 . For supertransients, one expects a power-law divergence in the exponent of the average lifetime, i.e.,

$$\tau(p, L) \sim \exp[c(L)(p_1 - p)^{-\delta}], \quad (32)$$

where $\delta > 0$ and the coefficient $c > 0$ depends on the system size L . Combining this with the size dependence of (19) or (21), we see that the coefficient a changes with parameter p as

$$a(p) \sim (p_1 - p)^{-\delta}. \quad (33)$$

A detailed investigation of the two-dimensional cGL equation (4) leads to the conclusion [3,39,40] that permanent spatiotemporal chaos is present in a region of the parameter plane (α, β) (μ fixed). When approaching the boundary of this region from outside, scaling (32) is found with exponent $\delta = 2$. Scaling law (32) is then similar to that valid in low-dimensional supertransient systems (cf. (9)), but exponent δ is found to be larger than unity, in contrast to χ , and a size dependence is also present.

When plotting the largest average Lyapunov exponent λ_f of the attractor as a function of parameter $p \equiv \alpha$, it is positive in a range $\alpha > \alpha_1$. Augmenting this figure with the largest Lyapunov exponent over the transients, the two curves merge smoothly (Fig. 8), illustrating that the spatiotemporal chaotic saddle is converted at α_1 into a chaotic attractor. The critical parameter value α_1 can thus be viewed as a point of external crisis in the cGL system. The Lyapunov exponent vanishes at some $\alpha_c < \alpha$, so the transients are not chaotic for $\alpha_c < \alpha$. The Lyapunov exponent around this point scales as $\lambda_f(\alpha) \sim (\alpha - \alpha_c)^{1/2}$ [3,39]. Interior crises of spatially extended systems will be discussed in the next subsections.

6.2. Interior crises in spatially coherent chaotic systems

A careful investigation of different types of crisis phenomena has been carried out in the KS equation by Rempel, Chian and coworkers [74–77]. These authors used form (3) of the equation in which the length is fixed but parameter ν contains the size of the original system. A parameter range was chosen for which the dynamics is chaotic in time but remains coherent in space. A Fourier decomposition of (3) with $N = 16$ modes appeared to be sufficient to illustrate the crisis phenomenon.

In a parameter range of ν a periodic window was found which can very well be seen by plotting the long time values of the sixth Fourier component a_6 as a function of ν . The window is bounded by an internal crisis and a saddle node bifurcation at its two ends (Fig. 9, left panel). The saddle-node bifurcation leads to the birth of two period-3 orbits, one attracting and the other unstable. It is this unstable periodic orbit which mediates the crisis at the other end of the window.

Inside the window the attractor is a period-3 orbit or is localized in three narrow bands. In both cases it is surrounded by an extended chaotic saddle. This surrounding chaotic saddle (SCS) has been determined by the PIM-triple method [78] and its projection on the a_6 variable is also shown in the bifurcation diagram. In the full phase space the chaotic saddle turns out to be extended but low-dimensional, as can be seen in a three-dimensional projection close to the saddle-node bifurcation, where no chaotic attractor exists. The saddle is practically a single line segment, but gaps are visible along this line (Fig. 9, right panel).

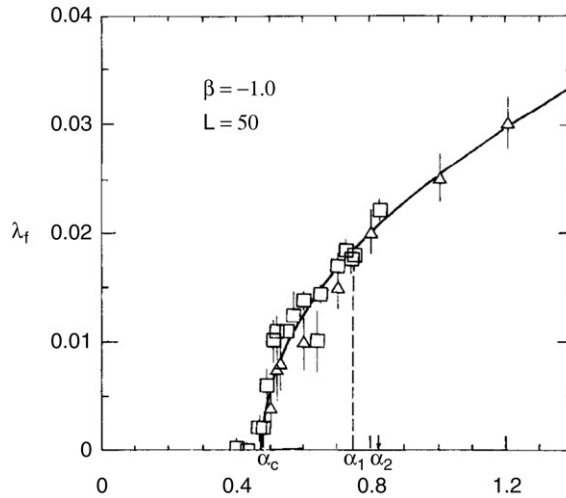


Fig. 8. The largest average Lyapunov exponent λ_f on the chaotic sets of the cGL equation (4) with $\mu = 0.2$, $\beta = -1$, $L = 50$ as a function of parameter α . Spatiotemporal chaos is permanent for $\alpha > \alpha_1$. For $\alpha_c < \alpha < \alpha_1$ only chaotic transients are present. Reprinted with permission from [39].

© 1990, by the American Physical Society, see <http://link.aps.org/abstract/PRA/v42/p3626>.

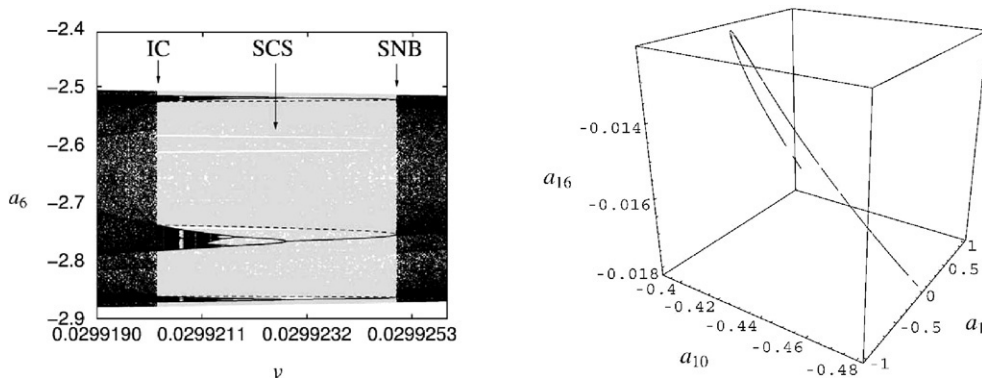


Fig. 9. Left: Bifurcation diagram in terms of mode amplitude a_6 as a function of parameter ν of the KS equation (3). Gray dots indicate points on the surrounding chaotic saddle (SCS). IC and SNB denote interior crisis and saddle-node bifurcation, respectively. Right: A three-dimensional projection of the SCS for $\nu = 0.029925$. From [75].

In the middle of the window the attractor undergoes a period doubling bifurcation after which a small-size chaotic attractor (CA), the three-band attractor, appears. The surrounding chaotic saddle, SCS, coexists now with the chaotic attractor. In a projection on the plane of two Fourier-components, one sees that the stable manifold of the mediating periodic orbit separates the attractor from the saddle (Fig. 10). The saddle’s stable manifold is also shown and appears to be rather dense in this projection.

At crisis, the small size chaotic attractor collides with the mediating orbit, and thus with the chaotic saddle as well (Fig. 11, left panel). The large gaps present along the surrounding saddle just before the crisis become filled up by newly generated orbits, and the extended chaotic attractor to appear contains both the previous attractor, the saddle, and the filled-up gaps (Fig. 11, right panel). After the crisis, points of the extended attractor which remain forever on the three bands occupied by the small attractor in the precrisis regime are connected to a saddle situated in this region, the band chaotic saddle (BCS). This saddle can be represented both on the bifurcation diagram (Fig. 12, left panel) and on a projection of the plane of two variables (Fig. 12, right panel). Similarly, points never leaving the region of the former surrounding chaotic saddle form a postcrisis chaotic saddle (SCS) which can be considered as the continuation of the precrisis SCS. These two saddles are the main building blocks of the extended chaotic attractor arising in

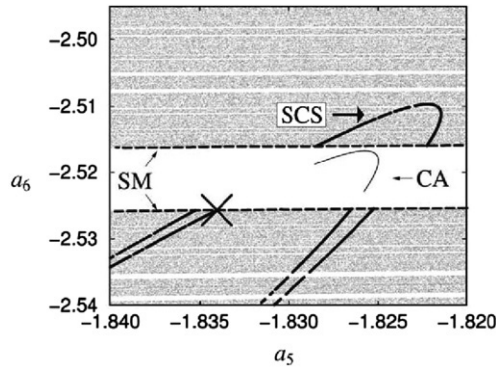


Fig. 10. Part of the phase space projected on the (a_5, a_6) plane for $\nu = 0.0299211$, before crisis. CA: chaotic attractor, SM: stable manifold of the mediating periodic orbit denoted by a cross. Grey dots mark the stable manifold of SCS. From [75].

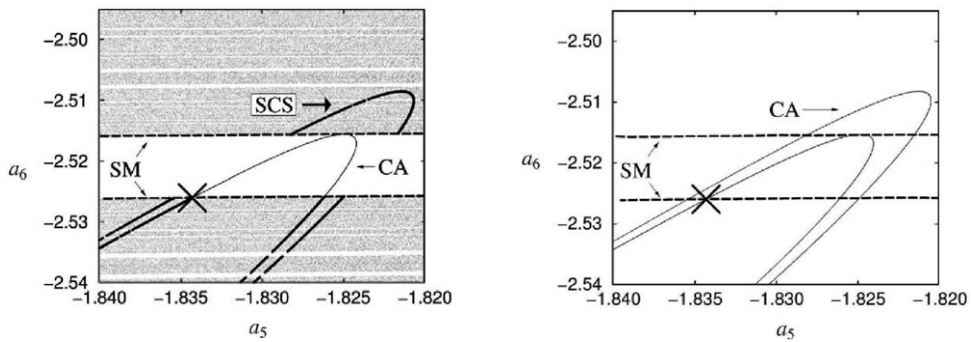


Fig. 11. Phase space projected on the (a_5, a_6) plane at IC, $\nu = 0.02992021$ (left panel), and slightly beyond crisis (right panel). From [75].

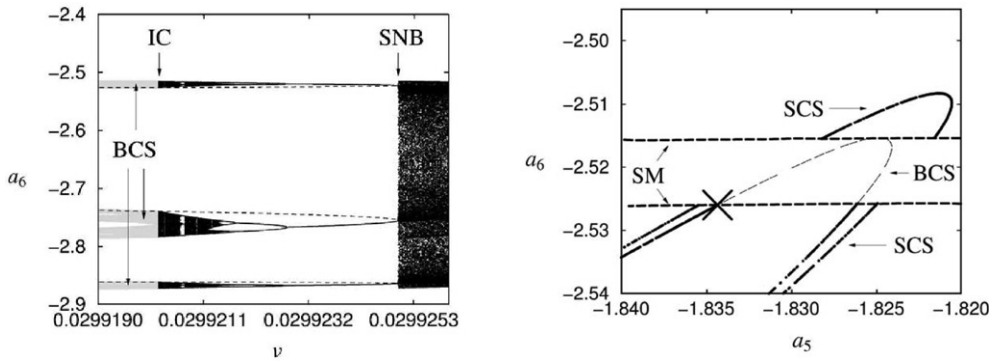


Fig. 12. Left: Bifurcation diagram as in Fig. 9 containing only the band chaotic attractor which is converted into a band chaotic saddle (BCS, plotted in gray) beyond IC. Right: Chaotic saddles forming the backbone of the extended chaotic attractor projected on the (a_5, a_6) plane at the postcrisis parameter $\nu = 0.02992006$. From [75].

the interior crisis. The situation is similar to what has been found in attractor explosions of low-dimensional maps [79–82]. This illustrates again that concepts developed for low-dimensional chaos can be applied to high dimensions.

6.3. Crises leading to fully developed spatiotemporal chaos

A recent paper of Rempel and Chian [83] aimed to understand crises underlying spatiotemporal inhomogeneities studied previously by He and Chian [84]. For this purpose they used a one-dimensional PDE model of regularized long waves for a field $\phi(x, t)$, which is driven sinusoidally both in space and time. With all other parameters fixed,

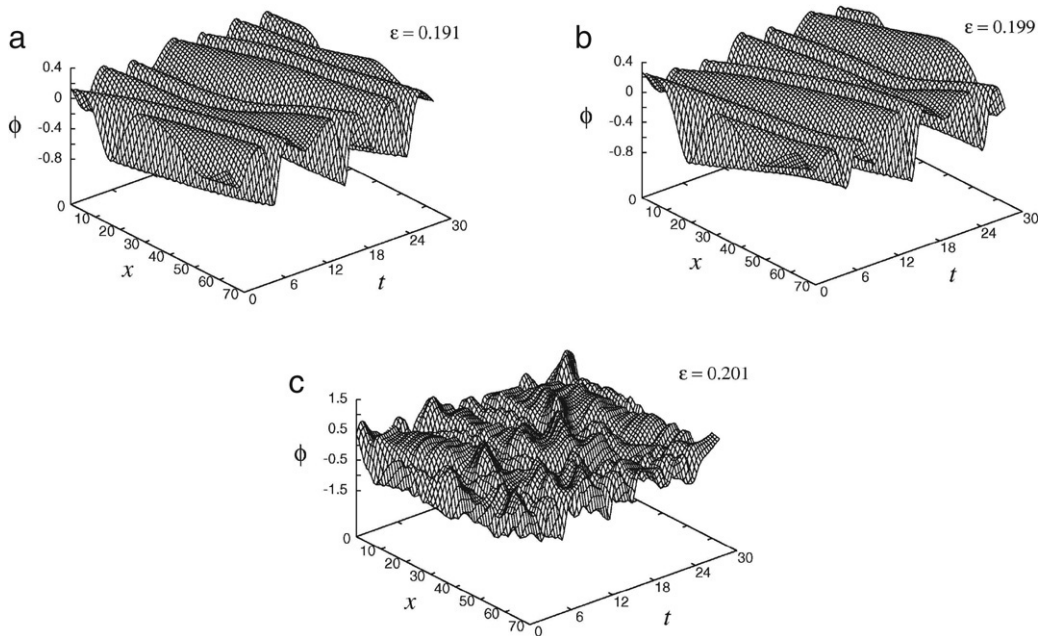


Fig. 13. Spatiotemporal patterns of field ϕ at different drivings, ϵ . (a): spatially regular, temporally quasiperiodic, (b): spatially regular, temporally chaotic, (c): spatially irregular, temporally chaotic. Reprinted with permission from [83].

© 2007, by the American Physical Society, see <http://link.aps.org/abstract/PRL/v98/p014101>.

the main control parameter is the driving amplitude ϵ . A Fourier decomposition of $\phi(x, t)$ into $N = 32$ spatial modes has been used. As ϵ is changed, the dynamics exhibit three qualitatively different types of behavior. At the lowest value of ϵ the pattern is regular in space and quasiperiodic in time [Fig. 13(a)]. At higher values, spatial regularity remains but the pattern becomes temporally chaotic [Fig. 13(b)], as indicated by the appearance of a positive Lyapunov exponent. The corresponding attractor is called the temporally chaotic attractor (TCA). A further increase in ϵ leads to the appearance of fully developed spatiotemporal chaos [Fig. 13(c)]. This occurs suddenly and is accompanied by a jump in the maximum Lyapunov exponent to a much larger value. The new attractor is the spatiotemporally chaotic attractor (STCA) that possesses a larger dimension value than the previous one (the TCA).

It is interesting to follow these changes in the phase space. Rempel and Chian projected the invariant sets on the plane defined by the real part of the second and of the third Fourier mode, after taking an appropriate Poincaré map. The quasiperiodic torus attractor appears to be associated with a few closed curves [Fig. 14(a)]. The authors pointed out that already here an extended chaotic saddle exists surrounding the attractor. The corresponding transients carry irregular spatiotemporal patterns, therefore the saddle is called the spatiotemporally chaotic saddle (STCS). When the spatially regular dynamics becomes chaotic, the torus attractor breaks, but the new temporally chaotic attractor (TCA) remains localized around the former torus [Fig. 14(b)]. The TCA is area-filling in the projection, but is of small size. The surrounding saddle, STCS, does not change too much. When permanent spatiotemporal chaos appears, the chaotic attractor suddenly broadens and becomes a spatiotemporally chaotic attractor, STCA [Fig. 14(c)]. It is remarkable that the extension of the STCA is practically the same as that of the spatiotemporal saddle (STCS) earlier. At this crisis the temporally chaotic attractor collides with the surrounding saddle, and the latter becomes embedded into the new attractor. In this postcrisis regime, Rempel and Chian were also able to identify a chaotic saddle on the region occupied by the temporal attractor earlier. This saddle is called therefore the temporally chaotic saddle (TCS) [Fig. 14(d)]. In the projection, it fills a slightly smaller area than the TCA.

If a trajectory on the extended attractor comes to the vicinity of the TCS, a regular pattern appears in the real space which changes chaotically in time. After some time, the trajectory deviates from this saddle, and comes close to the chaotic saddle that exists outside the TCS, a postcrisis STCS that governs the spatiotemporally chaotic dynamics. After an escape from here, the trajectory is around the TCS and the pattern becomes regular for a while again, etc. The average lifetime of the spatially regular phases can, in principle, be estimated as the average lifetime on the

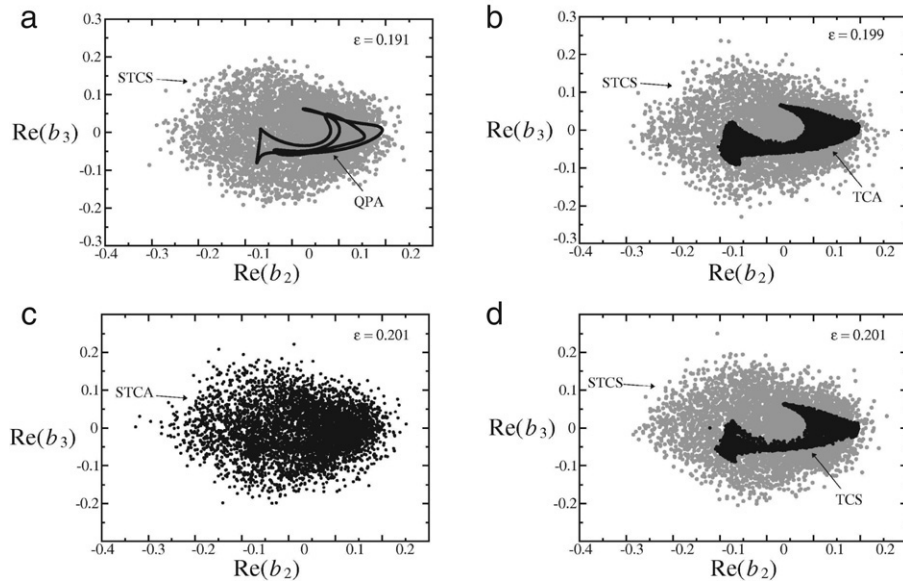


Fig. 14. Phase space projection on the plane of two modes. (a) A quasiperiodic attractor, QPA (black) and a spatiotemporally chaotic saddle, STCS (gray dots). (b) The STCS coexists with the temporally chaotic attractor, TCA, as well. (c) Beyond crisis, a spatiotemporally chaotic attractor, STCA, appears which occupies the space taken by the former STCS (and the TCA). (d) Beyond crisis, the STCA can be split into a postcrisis STCS and a temporally chaotic saddle, TCS. Reprinted with permission from [83].

© 2007, by the American Physical Society, see <http://link.aps.org/abstract/PRL/v98/p014101>.

TCS. The full process is intermittent, and the situation is the high-dimensional analog of what is called crisis induced intermittency in low-dimensional systems [85].

Spatiotemporal intermittency (STI) mentioned in Section 2.3 is not the kind of intermittency treated here since regular and irregular phases extend in STI over finite regions of the real space only. It might, nevertheless, be interesting to think about spatiotemporal intermittency in terms of the underlying chaotic saddles. At the moment very little is known about the scaling with system size of the lifetimes associated with the intermittent dynamics discussed here.

The scenario described in this subsection appears to be of a general nature since it has been demonstrated to apply to the damped KS equation [86] as well.

7. Fractal properties of supertransients

7.1. Partial dimension

Supertransients have very specific fractal properties. This feature was emphasized in [33,87–89]. It was observed that chaotic saddles underlying long transients typically have a stable manifold whose dimension is close to that of the phase space. The basin of attraction of the regular asymptotic attractor can be determined on a plane of initial conditions of just a few variables (Fig. 15a). In a long observation time only a few points converge to the attractor, the others remain away from it. These points represent initial conditions that stay close to a chaotic saddle's stable manifold. Alternatively, a plot of the lifetimes needed to reach the attractor as a function of a single initial coordinate also appears to be very dense (Fig. 15b). It is worth introducing a partial dimension d_s as the dimension of the set of points where the lifetime is formally infinite along such a segment. Since infinite lifetime values belong to the stable manifold of the saddle, this d_s is the dimension of the intersection of a line and of the stable manifold of the saddle.

As a quantitative measure of the fractality, the uncertainty exponent [6] was determined. Initial conditions of distance ϵ apart were taken from a line segment, and after a long time the local Lyapunov exponents were checked for all points. If in two neighboring points they turn out to be different, the interval in between is considered to be uncertain. The portion $f(\epsilon)$ of the uncertain intervals changes as $f(\epsilon) \sim \epsilon^\alpha$ with α being the uncertainty exponent. It is known to be related to the dimension d_s as $d_s = 1 - \alpha$. The numerical value of α was found to be as small as 10^{-3}

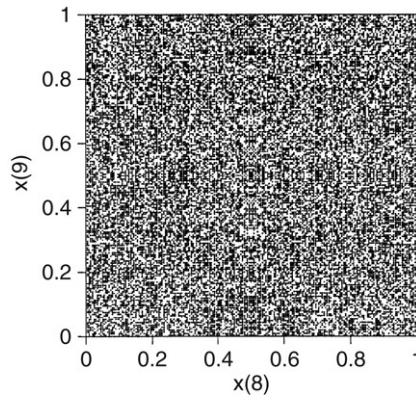


Fig. 15a. The stable manifold of a chaotic saddle (black dots) on the plane of two variables of a CML described by (1). Reprinted with permission from [33].

© 1995, by the American Physical Society, see <http://link.aps.org/abstract/PRL/v74/p5208>.

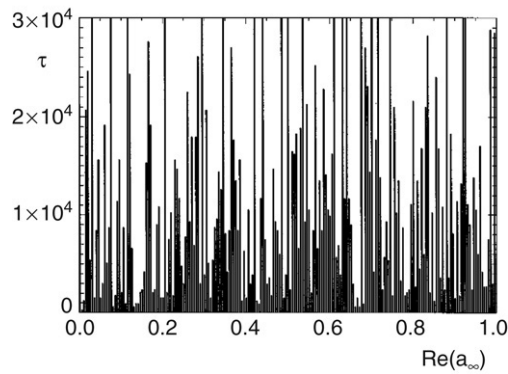


Fig. 15b. Transient lifetime as a function of the initial condition taken from a one-dimensional line in the phase space of the cGL equation in its supertransient state. The dimension of points with very large lifetimes on such plots is denoted by d_s . Reprinted with permission from [41].

© 1996, by the American Physical Society, see <http://link.aps.org/abstract/PRE/v53/p6562>.

(cf. Fig. 16), indicating that d_s is quite close to unity. It was also shown [87–89] that the largest Lyapunov exponent computed at a fixed finite time is extremely sensitive to tiny changes in the parameters. Therefore, supertransients are characterized by riddled structures in the parameter space as well.

In the context of dimensions, it is convenient to use, instead of the average lifetime, its reciprocal, the escape rate:

$$\kappa(L) = 1/\tau(L).$$

A simple formula for the partial dimension d_s was conjectured in [33]. In particular, since escape is slow, it is efficient along the direction of the largest positive Lyapunov exponent λ_{\max} only. The system is therefore expected to behave like a two-dimensional system with positive Lyapunov exponent λ_{\max} , and in view of the Kantz–Grassberger relation [90]

$$d_s(L) = 1 - \frac{\kappa(L)}{\lambda_{\max}}. \tag{34}$$

Taking into account that the dimension of a set resulting from the intersection of two sets follows from the rule according to which the codimensions are additive [91], one finds in an N -dimensional phase space that the dimension D_s of the stable manifold is

$$D_s(L) = N + d_s - 1 = N - \frac{\kappa(L)}{\lambda_{\max}}. \tag{35}$$

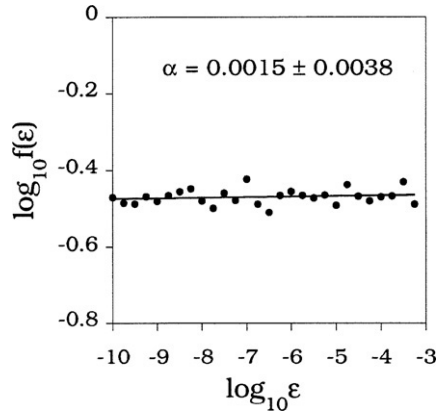


Fig. 16. Plot of the fraction of uncertain initial conditions $f(\epsilon)$ versus uncertainty ϵ . In view of the value of the uncertainty exponent α obtained, the dimension d_s is $d_s = 0.9985$, a quantity that is hardly distinguishable from 1. Reprinted with permission from [33]. © 1995, by the American Physical Society, see <http://link.aps.org/abstract/PRL/v74/p5208>.

The largest Lyapunov exponent can also depend on the system size. We do not expect, however, any drastic L dependence in λ_{\max} , and therefore this dependence is suppressed in the notation. Since κ is small, the dimension of the stable manifold is very close, for Type-II supertransients exponentially close, to the dimension of the phase space.

7.2. Application of general dimension formulae

It is worth pointing out that relation (35) immediately follows from a formula expressing the dimension of the stable manifold of an arbitrary high-dimensional saddle, derived by Hunt, Ott and Yorke [92], after the publication of expression (34) in Ref. [33]. In particular, consider a dynamical system described by an N -dimensional map. For a chaotic saddle in the N -dimensional phase space, there are $U > 0$ positive and $S > 0$ negative Lyapunov exponents, where $U + S = N$. Following Hunt et al. [92], we order the exponents, as follows:

$$\lambda_U^+ \geq \lambda_{U-1}^+ \geq \dots \lambda_1^+ > 0 \geq -\lambda_1^- \geq \dots \geq -\lambda_{S-1}^- \geq -\lambda_S^- \tag{36}$$

Thus, all quantities $\lambda_j^{+,-}$ are positive, and smaller values of the subscripts j correspond to Lyapunov exponents that are closer to zero in magnitude. The maximum Lyapunov exponent is λ_U^+ in this notation. Hunt et al. show that the dimension of the stable manifold of a generic chaotic saddle is

$$D_s = S + J + \frac{K - (\lambda_1^+ + \lambda_2^+ + \dots + \lambda_J^+)}{\lambda_{J+1}^+}, \tag{37}$$

where J is the largest index for which the denominator is still positive, i.e., the index for which

$$\lambda_1^+ + \lambda_2^+ + \dots + \lambda_J^+ + \lambda_{J+1}^+ \geq K \geq \lambda_1^+ + \lambda_2^+ + \dots + \lambda_J^+ \tag{38}$$

holds. Here

$$K = \sum_{j=1}^U \lambda_j^+ - \kappa \tag{39}$$

represents the metric entropy of the saddle.

Take now a spatiotemporal system with a small escape rate. When κ is nearly zero, the only option for the left-hand side of (38) to be larger than K , which contains the sum of all the positive Lyapunov exponents, is that all the positive Lyapunov exponents appear on the left hand side, i.e., $J + 1 = U$. The numerator of the ratio in (37) contains then $\lambda_U^+ - \kappa = \lambda_{\max} - \kappa$, and since $S + J = S + U - 1 = N - 1$, we recover (35).

It is also interesting to apply the dimension formula of other invariant sets. The general formula for the dimension of the unstable manifold of the saddle reads as [92]

$$D_u = U + I + \frac{K - (\lambda_1^- + \lambda_2^- + \cdots + \lambda_I^-)}{\lambda_{I+1}^-}, \quad (40)$$

where I is again the largest index for which the numerator is still positive, i.e., the index for which

$$\lambda_1^- + \lambda_2^- + \cdots + \lambda_I^- + \lambda_{I+1}^- \geq K \geq \lambda_1^- + \lambda_2^- + \cdots + \lambda_I^- \quad (41)$$

holds. The dimension of the chaotic saddle is obtained as

$$D = D_u + D_s - N. \quad (42)$$

When considering the case of spatiotemporal systems with small escape rate again, observe first that condition (41) requires that the sum of all Lyapunov exponents (with signs taken into account) up to index I is greater than κ , but up to index $I + 1$ it is smaller than κ . For κ nearly zero, these sums should practically be positive and negative, respectively. This is the condition in the Kaplan–Yorke formula [6] for chaotic attractors. One can then imagine a chaotic attractor with the same Lyapunov exponent spectrum as the saddle, and denote its Kaplan–Yorke dimension as D_{attr} . Given a discrete set of Lyapunov exponents, a small κ does not change the value of I , and we can write

$$D_u(L) = D_{\text{attr}} - \frac{\kappa(L)}{\lambda_{I+1}^-}. \quad (43)$$

For the saddle's dimension we then obtain, in view of (35),

$$D(L) = D_{\text{attr}} - \kappa(L) \left(\frac{1}{\lambda_{\text{max}}} + \frac{1}{\lambda_{I+1}^-} \right) = D_u(L) - \frac{\kappa(L)}{\lambda_{\text{max}}}. \quad (44)$$

Eqs. (35), (43) and (44) illustrate that a supertransient chaotic saddle is a *quasiattractor* in the sense that its dimension is very close to that of an attractor (with an identical Lyapunov spectrum), its stable manifold is nearly space-filling (it is very close to forming a basin of attraction), and its unstable manifold has nearly the same dimension as the chaotic saddle (for an attractor D_u and D should coincide). These observations show that the dimension of supertransient chaotic saddles can be approximated by the Kaplan–Yorke formula, and explain in other terms why statistical averages are so well defined on supertransient chaotic saddles.

It is worth mentioning that although the stable manifold is nearly space filling, the unstable manifold's dimension can take on any value. It is the number U of positive Lyapunov exponents and the index I which essentially determines the value of D_u . In principle it can assume a small value even in a high-dimensional phase space.

7.3. Dimension densities

In high-dimensional systems it is natural to define dimension densities [3,28,22], i.e., a quantity expressing the dimension falling on a single degree of freedom. The dimension density $\delta_s \equiv D_s/N$ of the stable manifold is for supertransients quite close to unity.

Little is known, however, about the dimension density $\delta_u = D_u/N$ and $\delta = D/N$ of the unstable manifold and of the saddle, respectively. The question so far has been addressed in a single supertransient system only. In particular, for a model of excitable media Strain and Greenside [49] found the dimension density of the chaotic set to be rather low. This is also consistent with an observation in RD systems [42] according to which the number of positive Lyapunov exponents is small even in large systems (although the number increases with the system size).

An important dynamical property in many high-dimensional systems is the existence of a Lyapunov density [3]. It implies that the set of the Lyapunov exponents λ_j^\pm as a function of $x \equiv j/N$ converges for $N \rightarrow \infty$ to a well-defined function $A^\pm(x)$ on the unit interval, as illustrated by Fig. 17. In such cases the number of positive (or negative) Lyapunov exponents scales with the dimension of the phase space, and U/N converges to a constant. As a result,

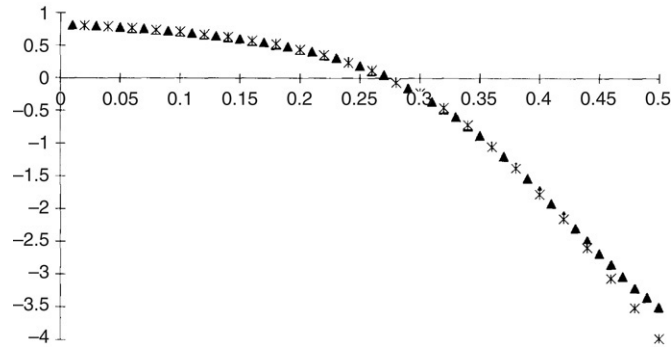


Fig. 17. The spectrum of Lyapunov exponents λ_j of the chaotic transients of a CML of length $N = 50$ (crosses) and $N = 100$ (triangles), as a function of j/N . The convergence to a limiting Lyapunov density can be seen. From [28].

e.g., the metric entropy (39) can be written as

$$K = \int_0^{U/N} \Lambda^+(x) dx - \kappa. \quad (45)$$

Similarly, the sums defining the indices J and I [see (38) and (41)], more precisely, the ratios J/N and I/N can also be expressed as integrals, which depend on the value of the escape rate. For small escape rates, however, the dependence becomes negligible, and we have $J/N = (U - 1)/N \rightarrow U/N$. Since the fraction appearing in the general expression of D_s and D_u is always less than one, it does not contribute to the dimension density. We thus find that supertransients are characterized by the following dimension densities:

$$\delta_s = \frac{S + U}{N} = 1, \quad \delta = \delta_u = \frac{U + I}{N}. \quad (46)$$

In view of relation (41), the nontrivial dimension density $\delta_u = \delta$ fulfills the equation

$$\int_0^{\delta_u} \Lambda(x) dx = 0, \quad (47)$$

where Λ denotes the signed Lyapunov density as seen in Fig. 17 ($\Lambda(x) = \Lambda^+(U/N - x)$ for $x \leq U/N$ and $\Lambda(x) = -\Lambda^-(x - U/N)$ for $x > U/N$). When considering the integral of the signed Lyapunov density between zero and some x , the dimension density is the x value for which the integral vanishes. In fact, relation (47) is valid for spatiotemporal chaotic attractors as well [93]. In summary, the picture based on Lyapunov and dimension densities suppresses the role of the finite lifetime of chaos, and emphasizes the quasiattractor character of supertransients.

8. Turbulence in pipe flows

8.1. Turbulence lifetime

The transition to turbulence in pipe flows has long been a fascinating problem in fluid dynamics (for reviews, see [94,95]). Investigations of the phenomenon started in the second part of the nineteenth century with the milestone experiments of Reynolds in 1883. He pointed out that in a pipe of fixed length the flow changes from smooth (laminar) to irregular (turbulent) at sufficiently large flow velocities. A good dimensionless measure of the flow velocity turns out to be the Reynolds number defined in (7) with U and D chosen as the mean flow speed across the pipe and the diameter, respectively. When slowly increasing the flow velocity in a given setting, the transition from laminar flow to turbulence occurs abruptly, at a critical Reynolds number, Re_c , which is of the order of 2000. Already the early experiments indicated, however, that under very carefully controlled conditions the laminar flow can be maintained up to Reynolds numbers much larger than 2000. Later it turned out that the roughness of the wall's surface plays an important role: the rougher the wall, the smaller the critical Reynolds number. More recent investigations have led to the observation that an initial disturbance of the laminar flow (a special case of which is the effect of surface

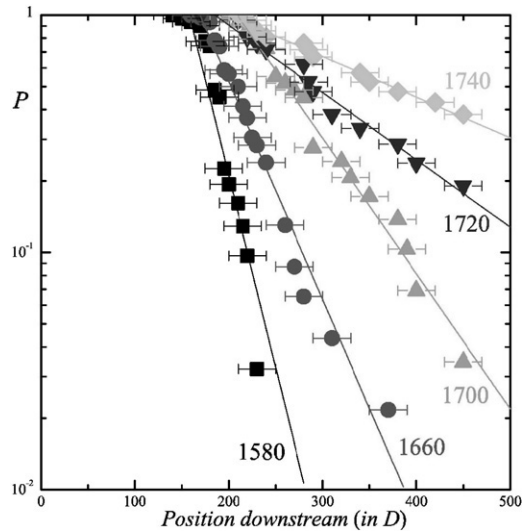


Fig. 18. Probability of observing a turbulent puff as a function of the dimensionless downstream distance from the point where the puff is generated in an experiment. The numbers along the graphs denote the Re values. The average lifetime increases with the Reynolds number. Reprinted with permission from [97].

© 2006, by the American Physical Society, see <http://link.aps.org/abstract/PRL/v96/p094501>.

roughness) is needed to trigger turbulence, and the critical Reynolds number Re_c depends on the type and the strength of the disturbance. Thus the onset of turbulence is determined not only by the Reynolds number but also by the disturbance. To trigger turbulence, the flow has to be sufficiently fast and the perturbation has to be sufficiently strong. The required perturbation is, however, the smaller the larger the Reynolds number. Therefore, in any experimental setting, where small perturbations cannot be avoided, turbulence will always appear at sufficiently large Reynolds number.

A characteristic feature of pipe flows is that the steady laminar solution, such as the parabola profile in a pipe of circular cross section, is linearly stable for *all* Reynolds numbers [94]. In dynamical-system terms, this implies that there is a fixed-point attractor in the infinite dimensional phase space, with a relatively small basin of attraction. In addition, there is no evidence for the existence of any stable state with simple spatial or temporal pattern. In other words, there are no other regular attractors that are, e.g., the analogs of limit cycles. The turbulent state can be considered as a high-dimensional chaotic state which can be associated with either a chaotic attractor or a chaotic saddle.

The first indications on the transient character of pipe turbulence appeared about twenty years ago [96,94], based on the stability investigation of the laminar profile. There has been increasing experimental evidence since then indicating that even if the turbulent state is established at not too large Reynolds numbers, this state can suddenly decay, without any clear precursor, towards the laminar state. This implies that the chaotic set at not too large Reynolds numbers is nonattracting, i.e., a chaotic saddle. Research has then been concentrated on the average lifetime τ of the chaotic saddle. In view of the classical experiments, it becomes clear that the lifetime must be rather large, for otherwise, the turbulence could not have appeared to be permanent for earlier investigators. The use of long pipes and efficient numerical codes have made more detailed investigations possible. For instance, Peixinho and Mullin followed turbulent puffs downstream and measured the position along the pipe where they relaminarize [97]. The distributions were found to be exponentially decaying as shown in Fig. 18. With length and time units D and D/U respectively, the dimensionless distance and dimensionless time to reach this distance are proportional to each other (i.e., the dimensionless velocity is of the order of unity). One thus concludes that the slope of the exponential decay of the probability to find a turbulent puff of lifetime of at least t is proportional to the escape rate $\kappa = 1/\tau$. This value appears to be *independent* of the details of the initial perturbation, but depends of course on the Reynolds number. As Fig. 18 illustrates, the exponential decay sets in after some time t_0 only, in any experimental run.

When plotting the actual lifetime as a function of the perturbation amplitude A to trigger the turbulence in numerical simulations, a more detailed picture can be obtained. A slight change in the amplitude can lead to drastically different

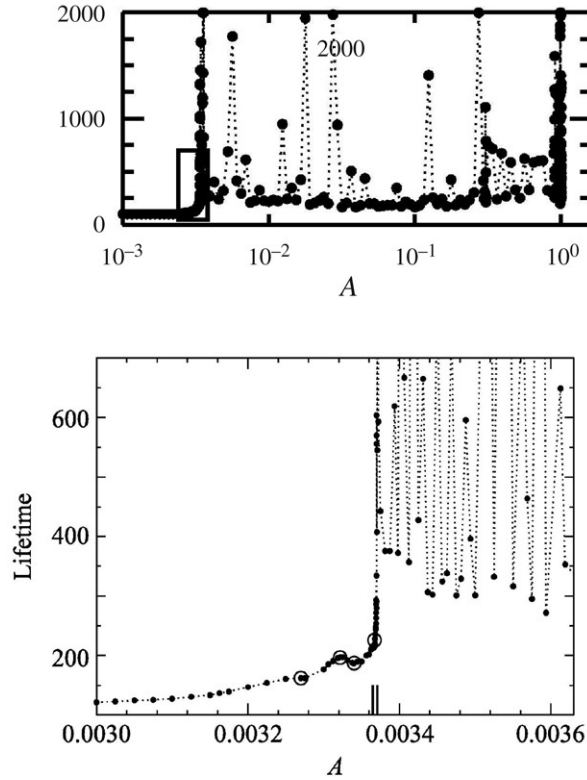


Fig. 19. Turbulence lifetime versus perturbation amplitude A in a pipe at Reynolds number $Re = 2000$ obtained in a numerical simulation. The bottom panel is a magnification of the box indicated in the top panel. At the edge of chaos, at the value marked by two vertical bars, the function turns from smooth to fractal like, a hint on the chaoticity of the transients triggered by sufficiently large amplitudes. From [53].

lifetimes, if the amplitude is above a threshold (Fig. 19). The irregular part of the lifetime distribution is fractal (cf. Fig. 19 lower panel). Furthermore, the average Lyapunov exponent during the turbulent phase has been shown to be strictly positive [53]. These features indicate that the high-dimensional saddle underlying the turbulence has all the characteristics of low-dimensional chaotic saddles and of transient chaos in many other spatiotemporal systems.

A basic question concerns the dependence of the turbulent lifetime on the Reynolds number. In the class of functions exhibiting a rapid increase with the Reynolds number, one option has been a function approaching infinity at a finite value of Re . This form can retain one aspect of the original picture, namely that beyond a threshold Reynolds number permanent turbulence can be present. The laminar fixed point attractor would then coexist with the chaotic attractor of the turbulence. The other option has been a monotonically increasing function of Re with finite values at any finite Re . Up to the last few years, the first candidate had appeared to be more reasonable.

By using a pipe of length 30 m, the very recent experiments by Hof, Westerweel, Schneider and Eckhardt [54, 95] seem to have provided a firm answer to the question. In a set of experiments covering more than two decades of lifetimes, Hof et al. showed that the average lifetime does not diverge, but rather increases exponentially with the Reynolds number. By measuring time in units of D/U , the dimensionless lifetime is found to scale with Re as

$$\tau(Re) = e^{bRe-a} \quad (48)$$

with parameters $a = 59.3$, $b = 0.034$ (see Fig. 20). Note that any increase of the Reynolds number by 100 implies a multiplication of the average lifetime by a factor of 30. Thus, pipe turbulence is a kind of Type-II supertransients (with system size replaced by the Reynolds number).

As an application of the fractal characteristics derived in Section 7, we conclude, based on (34), that the deviation of the partial dimension d_s of the intersection between a line and the stable manifold of the saddle from unity scales

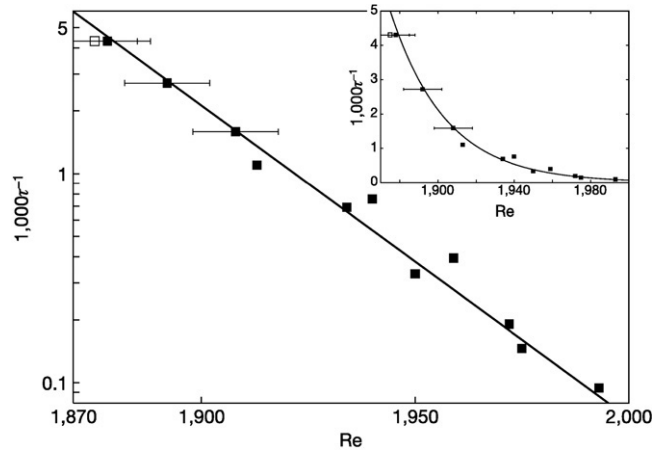


Fig. 20. The escape rate, τ^{-1} , as a function of the Reynolds number in the experiment by Hof et al. The straight line fit corresponds to formula (48). The inset shows the same data on a linear scale to illustrate that the escape rate asymptotes to zero rather than crossing the horizontal axis at a finite value of Re . Reprinted with permission from the Annual Review of Fluid Mechanics, Volume 39 [95].

© 2007, by Annual Reviews www.annualreviews.org.

with the Reynolds number as

$$1 - d_s(Re) \sim e^{a-bRe}. \quad (49)$$

Here we have assumed that the largest dimensionless Lyapunov exponent depends only weakly on the Reynolds number.

8.2. Other aspects of hydrodynamical supertransients

An interesting feature of the lifetime distribution versus perturbation amplitude as shown in Fig. 19 is that slowly varying regions are interwoven with intervals of rapid change. In the smooth regions the transients are short and nonchaotic. The transition (indicated by two bars in Fig. 19) between the extended smooth region at small amplitudes and the region with fractal fluctuations is rather abrupt. This point on the border between laminar and chaotic regions is called the edge of chaos [98,99]. The edge of chaos separates thus initial conditions that decay directly to the laminar attractor and those that come close to the chaotic saddle first, i.e., exhibit turbulence. Trajectories starting from the edge of chaos move in a region intermediate between laminar and turbulent dynamics. The results of [98,99] suggest that the edge of chaos lies, at any Reynolds number, on the stable manifold of an invariant object that resides in the phase space between the fixed point and the chaotic saddle. This stable manifold is a kind of basin boundary between the laminar and turbulent dynamics. The latter, of course, cannot have a real basin of attraction, but only one which appears to be so in finite time observations (see the quasiattractor character discussed in Section 7). The dynamics restricted to the edge of chaos converges to a chaotic state, and the first numerical simulations in pipe flows indicate that it corresponds indeed to an irregular wavy motion along the pipe which is, however, less energetic than the turbulent dynamics itself [99]. This attractor is, of course, only a relative attractor since it is unstable with respect to perturbations perpendicular to the edge of chaos.

Low-dimensional chaotic saddles are known to contain an infinite number of unstable periodic orbits. In an analogous way, the chaotic saddle underlying pipe turbulence is expected to contain so-called coherent structures. They are shown to be regular traveling waves [52,100], all *unstable*, corresponding to hyperbolic states in the high-dimensional phase space. Currently, there is an intensive search for such coherent structures [101–103], about which chaos is organized. Over a long-time observation of turbulence one expects to see different coherent states in different time intervals. This kind of approach might eventually lead to a periodic orbit expansion of the chaotic saddle, in full analogy with low-dimensional problems [104,105]. There is then hope that the statistical properties of the turbulent flow might be expressed in terms of the properties of the coherent structures.

Finally we mention that there are other hydrodynamical situations where the onset of turbulence is similar to that in pipe flows. Notable examples are plane Poiseuille flows (pressure-driven flows in between two large parallel

plates) [106] and Couette flows (driven by a moving wall) [107–109]. The common feature in these shear flows is that the laminar profile is not unstable. One expects therefore in these situations that turbulence is not permanent, it decays eventually towards a laminar profile. Shear-flow turbulence is thus a case of its own, and is present in the form of high-dimensional chaotic transients. We are thus currently witnessing the appearance of concepts of transient chaos in the study of classical turbulence.

9. Discussions

Our review has been focused on supertransients. Although they are quite common, there are cases where the distribution of transient lifetimes is not exponential, or if it is, the average lifetime does not grow rapidly with the system size. It might, e.g., become saturated (for examples see [110,22]). The type of coupling plays an important role [111]. It is, nevertheless, an open question at the moment if one can decide from first principles (by merely looking at the dynamical equations) whether a system with spatiotemporal transients exhibits a supertransient or a different kind of scaling. In fact, the even simpler question of how to decide if a spatiotemporal system possesses a chaotic attractor is also complex. Here a systematic application of a nonlinear stability analysis to different possible asymptotic patterns [43] might provide an answer. A recent investigation [48] shows that the master stability function [112], a central tool in the theory of synchronization of dynamical systems [113], can successfully be applied as an indicator for transient versus permanent spatiotemporal chaos.

A somewhat analogous phenomenon to supertransients has been found in Hamiltonian systems with many degrees of freedom. Any isolated macroscopic system should eventually relax to a state of thermal equilibrium where any macroscopic variable is independent of time. Nevertheless, in systems with global (mean field) coupling long relaxations have been found whose average time diverges with the number of components [114–117]. More recently, a metastable state has been discovered [118] which is characterized by a periodic or quasiperiodic oscillation of macroscopic variables around a mean different from the equilibrium value. The lifetime of the metastable state is found to increase linearly with the number of degrees of freedom. The underlying, microscopic dynamics is, of course, chaotic, but must be in some sense of a different nature in the metastable and in the equilibrium state. Both examples can be considered as Type-I supertransients, which last very long in the thermodynamic limit.

The problem of stable chaos (Section 4.4) deserves renewed attention. Although these systems appear to exhibit fractal features, dimension formulae (37) and (40) cannot be applied to them. In fact, these relations are valid for generic chaotic saddles, which is not the case here. It would, therefore, be of interest to know more about these systems, which might turn out to have an underlying strange nonchaotic spatiotemporal saddle. Strange nonchaotic repellers of one-dimensional maps have recently been described by de Moura [119] (in some analogy with strange nonchaotic attractors [120]). Strange nonchaotic spatiotemporal saddles might have a fractal dimension not increasing linearly with the system size, i.e., having a density $\delta_u = \delta = 0$.

In some spatiotemporal problems the linear size cannot be freely chosen. Long transients might, nevertheless, be present (see e.g. [121,122]) but it is not obvious whether they scale at all with some parameter of the problem. In a pattern of falling liquid columns, for instance, a spatiotemporal intermittency (STI) like behavior has been found which proved to be transient in a certain parameter range with a lifetime scaling according to Eq. (8) [123]. It is worth trying to find a scaling parameter in such cases as well and check if the dependence is a power law or an exponential. In the case of time-delayed systems [121] a natural candidate for some scaling parameter could be the delay time.

It is worth pointing out a slight difference between the shear-turbulence problem and supertransient phenomena in other spatially extended systems. The scaling in turbulence is not with respect to the length of the pipe, rather with the diameter [contained in the Reynolds number (7)]. It would be interesting to better understand this difference, e.g., by checking how the lifetime of turbulent puffs changes with their own extension along the pipe. On the other hand, the level of analysis applied seems to be more advanced for turbulence than in other cases. The concept of unstable coherent structures as building blocks for a periodic-orbit type of expansion of the chaotic saddle, or that of the edge of chaos and the invariant sets associated with it, might usefully be applied to all other systems exhibiting supertransients. It is quite remarkable that problems ranging from fluid dynamics and chemistry to population dynamics and biology (with quite different underlying mathematical structures) all share similar features, dominated by long-lasting chaotic transients. A unified understanding of the physics underlying this phenomenon deserves further efforts.

Acknowledgements

The authors are indebted for useful discussion with A. Chian, B. Eckhardt, K. Kaneko, A. Politi, E. Rempel, K. Showalter, E. Schöll, J. Vollmer and R. Wackerbauer. Special thanks are due to our colleagues, and the publishers, the American Physical Society, the Annual Reviews, Cambridge University Press, EDP sciences, and Elsevier, who permitted the use of their figures. This research was supported by the OTKA grant T047233. YCL was supported by AFOSR under Grant No. FA9550-06-1-0024.

References

- [1] K. Kaneko, *Theory and Applications of Coupled Map Lattices*, Wiley, Chichester, 1993.
- [2] S. Wolfram, *Cellular Automata and Complexity*, first edn, Addison-Wesley, Reading, MA, 1994.
- [3] T. Bohr, M.H. Jensen, G. Paladin, A. Vulpiani, *Dynamical Systems Approach to Turbulence*, Cambridge University Press, Cambridge, 1998.
- [4] P. Manneville, *Instabilities, Chaos and Turbulence*, Imperial College Press, Cambridge, 2004.
- [5] K. Kaneko, I. Tsuda, *Complex Systems: Chaos and Beyond, A Constructive Approach with Applications in Life Sciences*, Springer, Berlin, 2000.
- [6] E. Ott, *Chaos in Dynamical Systems*, Cambridge University Press, Cambridge, 1993.
- [7] T. Tél, M. Gruiz, *Chaotic Dynamics: An Introduction Based on Classical Mechanics*, Cambridge University Press, Cambridge, 2006.
- [8] C. Grebogi, E. Ott, J.A. Yorke, Fractal basin boundaries, long-lived chaotic transients, and unstable–unstable pair bifurcation, *Phys. Rev. Lett.* 50 (1983) 935–938.
- [9] A. Politi, R. Livi, G.L. Oppo, R. Kapral, Unpredictable behaviour in stable systems, *Europhys. Lett.* 22 (1993) 571–576.
- [10] K. Kaneko, Spatiotemporal intermittency in coupled map lattices, *Progr. Theoret. Phys.* 74 (1985) 1033–1044.
- [11] J.D. Keeler, J.D. Farmer, Robust space–time intermittency and $1/f$ noise, *Physica D* 23 (1986) 413–435.
- [12] H. Chaté, P. Manneville, Transition to turbulence via spatiotemporal intermittency, *Phys. Rev. Lett.* 58 (1987) 112–115.
- [13] H. Chaté, P. Manneville, Spatio-temporal intermittency in coupled map lattices, *Physica D* 32 (1988) 409–422.
- [14] K. Kaneko, Pattern dynamics in spatiotemporal chaos, *Physica D* 34 (1989) 1–41.
- [15] J.P. Gollub, Order and disorder in fluid motion, *Proc. Natl. Acad. Sci. USA* 92 (1995) 6705–6711.
- [16] P. Rupp, R. Richter, I. Rehberg, Critical exponents of directed percolation in spatiotemporal intermittency, *Phys. Rev. E* 67 (2003) 036209.
- [17] V. Lepiller, A. Prigent, F. Dumochel, I. Mutabazi, Transition to turbulence in a tall annulus submitted to a radial temperature gradient, *Phys. Fluids* 19 (2007) 054101.
- [18] P. Grassberger, T. Schneider, Phase transitions in coupled map lattices, *Physica D* 50 (1991) 177–188.
- [19] J.C. Alexander, J.A. Yorke, Z. You, I. Kan, Riddled basins, *Internat. J. Bifur. Chaos Appl. Sci. Engrg.* 2 (1992) 795–813.
- [20] Y.-C. Lai, C. Grebogi, J.A. Yorke, S. Venkataramani, Riddling bifurcation in chaotic dynamical systems, *Phys. Rev. Lett.* 77 (1996) 55–58.
- [21] Zhilin Qu, Gang Hu, Spatiotemporal periodic states, periodic windows, and intermittency in coupled-map lattices, *Phys. Rev. E* 49 (1994) 1099–1108.
- [22] F.H. Willeboordse, Supertransients and suppressed chaos in the diffusively coupled logistic lattice, *Chaos* 89 (1994) 89–98.
- [23] C. Grebogi, E. Ott, J.A. Yorke, Chaotic attractors in crisis, *Phys. Rev. Lett.* 48 (1982) 1507–1510.
- [24] C. Grebogi, E. Ott, J.A. Yorke, Crises, sudden changes in chaotic attractors and chaotic transients, *Physica D* 7 (1983) 181–200.
- [25] C. Grebogi, E. Ott, J.A. Yorke, Super persistent chaotic transients, *Ergodic Theory Dynam. Systems* 5 (1985) 341–372.
- [26] G. Ahlers, R. Walden, Turbulence near onset of convection, *Phys. Rev. Lett.* 44 (1980) 445–448.
- [27] J.P. Crutchfield, K. Kaneko, Are attractors relevant to turbulence?, *Phys. Rev. Lett.* 60 (1988) 2715–2718.
- [28] R. Livi, G. Martinez-Mekler, S. Ruffo, Periodic orbits and long transients in coupled map lattices, *Physica D* 45 (1990) 452–460.
- [29] S.V. Ershov, A.B. Potapov, On the nature of nonchaotic turbulence, *Phys. Lett. A* 167 (1992) 60–64.
- [30] R. Kapral, R. Livi, G.L. Oppo, A. Politi, Dynamics of complex interfaces, *Phys. Rev. E* 49 (1994) 2009–2022.
- [31] A. Politi, A. Torcini, Linear and non-linear mechanism of information propagation, *Europhys. Lett.* 28 (1994) 545–550.
- [32] K. Kaneko, Supertransients, spatiotemporal intermittency and stability of fully developed spatiotemporal chaos, *Phys. Lett. A* 149 (1990) 105–112.
- [33] Y.-C. Lai, R.L. Winslow, Geometric properties of the chaotic saddle responsible for supertransients in spatiotemporal chaotic dynamical systems, *Phys. Rev. Lett.* 74 (1995) 5208–5211.
- [34] L.A. Bunimovich, Ya.G. Sinai, Spacetime chaos in coupled map lattices, *Nonlinearity* 1 (1988) 491–516.
- [35] A. Wacker, S. Bose, E. Schöll, Transient spatio-temporal chaos in a reaction–diffusion model, *Europhys. Lett.* 31 (1995) 257–262.
- [36] S. Scott, B. Peng, A. Tomlin, K. Showalter, Transient chaos in a closed chemical-system, *J. Chem. Phys.* 94 (1991) 1134–1140.
- [37] B. Shraiman, Order, disorder, and phase turbulence, *Phys. Rev. Lett.* 57 (1986) 325–328.
- [38] J. Hyman, B. Nicolaenko, S. Zaleski, Order and complexity in the Kuramoto–Sivashinsky model of weakly turbulent interfaces, *Physica D* 23 (1986) 265–292.
- [39] T. Bohr, A.W. Pedersen, M.H. Jensen, Transition to turbulence in a discrete Ginzburg–Landau model, *Phys. Rev. A* 42 (1990) 3626–3629.
- [40] G. Huber, P. Alstrom, T. Bohr, Nucleation and transients at the onset of vortex turbulence, *Phys. Rev. Lett.* 69 (1992) 2380–2383.
- [41] R. Braun, F. Feudel, Supertransient chaos in the two-dimensional complex Ginzburg–Landau equation, *Phys. Rev. E* 53 (1996) 6562–6565.
- [42] M. Meixner, S. Bose, E. Schöll, Analysis of complex and chaotic patterns near a codimension-2 Turing–Hopf point in a reaction-diffusion model, *Physica D* 109 (1997) 128–138.

- [43] M. Meixner, A. De Wit, S. Bose, E. Schöll, Generic spatiotemporal dynamics near codimension-2 Turing–Hopf bifurcations, *Phys. Rev. E* 55 (1997) 6690–6697.
- [44] M. Meixner, S.M. Zoldi, S. Bose, E. Schöll, Karhunen-Loeve local characterization of spatiotemporal chaos in a reaction-diffusion system, *Phys. Rev. E* 61 (2000) 1382–1385.
- [45] R. Wackerbauer, K. Showalter, Collapse of spatiotemporal chaos, *Phys. Rev. Lett.* 91 (2003) 174103.
- [46] S. Yonker, R. Wackerbauer, Nonlocal coupling can prevent the collapse of spatiotemporal chaos, *Phys. Rev. E* 73 (2006) 026218.
- [47] R. Wackerbauer, S. Kobayashi, Noise can delay and advance the collapse of spatiotemporal chaos, *Phys. Rev. E* 75 (2007) 066209.
- [48] R. Wackerbauer, Master stability analysis in transient spatiotemporal chaos, 2007. Preprint.
- [49] M.C. Strain, H.S. Greenside, Size-dependent transition to high-dimensional chaotic dynamics in a two-dimensional excitable medium, *Phys. Rev. Lett.* 80 (1998) 2306–2309.
- [50] A. Zumdieck, M. Timme, T. Geisel, F. Wolf, Long chaotic transients in complex networks, *Phys. Rev. Lett.* 93 (2004) 244103.
- [51] R. Zillmer, R. Livi, A. Politi, A. Torcini, Desynchronization in diluted neural networks, *Phys. Rev. E* 74 (2006) 036203.
- [52] F. Faisst, B. Eckhardt, Traveling waves in pipe flow, *Phys. Rev. Lett.* 91 (2003) 224502.
- [53] F. Faisst, B. Eckhardt, Sensitive dependence on initial conditions in transition to turbulence in pipe flow, *J. Fluid. Mech.* 504 (2004) 343–352.
- [54] B. Hof, J. Westerweel, T.M. Schneider, B. Eckhardt, Finite lifetime of turbulence in shear flows, *Nature* 443 (2006) 59–62.
- [55] F.A. Bignone, Cells–genes interaction simulation on a coupled map lattice, *J. Theoret. Biol.* 161 (1993) 231–249.
- [56] Y. Cuche, R. Livi, A. Politi, Phase transitions in 2d linearly stable coupled map lattices, *Physica D* 103 (1997) 369–380.
- [57] A. Torcini, P. Grassberger, A. Politi, Error propagation in extended systems, *J. Phys. A* 27 (1995) 4533–4541.
- [58] F. Cecconi, R. Livi, A. Politi, Fuzzy transition region in a one-dimensional coupled-stable-map lattice, *Phys. Rev. E* 57 (1998) 2703–2712.
- [59] F. Ginelli, R. Livi, A. Politi, Emergence of chaotic behaviour in linearly stable systems, *J. Phys. A* 35 (2002) 499–516.
- [60] R. Bonaccini, A. Politi, Chaotic-like behaviour in chains of stable nonlinear oscillators, *Physica D* 103 (1997) 362–368.
- [61] P. Cipriani, S. Denisov, A. Politi, From anomalous energy diffusion to Levy walks and heat conductivity in one-dimensional systems, *Phys. Rev. Lett.* 94 (2005) 244301.
- [62] L. Delfini, S. Denisov, S. Lepri, R. Livi, P.K. Mohanty, A. Politi, Energy diffusion in hard-point systems, *Eur. Phys. J. Special Topics* 146 (2007) 21–35.
- [63] C.W. Gardiner, *Handbook of Stochastic Methods*, first edn, Springer-Verlag, New York, 1997.
- [64] H. Risken, *The Fokker–Planck Equation*, first edn, Springer-Verlag, Berlin, 1989.
- [65] Y. Do, Y.-C. Lai, Extraordinarily superpersistent chaotic transients, *Europhys. Lett.* 67 (2004) 914–920.
- [66] Y. Do, Y.-C. Lai, Scaling laws for noise-induced superpersistent chaotic transients, *Phys. Rev. E* 71 (2005) 046208.
- [67] V. Andrade, R. Davidchack, Y.-C. Lai, Noise scaling of phase synchronization of chaos, *Phys. Rev. E* 61 (2000) 3230–3233.
- [68] M.G. Rosenblum, A.S. Pikovsky, J. Kurths, Phase synchronization of chaotic oscillators, *Phys. Rev. Lett.* 76 (1996) 1804–1807.
- [69] Y. Do, Y.-C. Lai, Superpersistent chaotic transients in physical space: Advective dynamics of inertial particles in open chaotic flows under noise, *Phys. Rev. Lett.* 91 (2003) 224101.
- [70] I.J. Benczik, Z. Toroczkai, T. Tél, Selective sensitivity of open chaotic flows on inertial tracer advection: Catching particles with a stick, *Phys. Rev. Lett.* 89 (2002) 164501.
- [71] Y.-C. Lai, Persistence of supertransients of spatiotemporal chaotic dynamics in noisy environment, *Phys. Lett. A* 200 (1995) 418–422.
- [72] M. Franaszek, Influence of noise on the mean lifetime of chaotic transients, *Phys. Rev. A* 44 (1991) 4065–4067.
- [73] P. Reimann, Noisy one-dimensional maps near a crisis II: general uncorrelated white noise, *J. Stat. Phys.* 85 (1996) 403–425.
- [74] A.C. Chian, E.L. Rempel, E.E. Macau, R.R. Rosa, F. Christiansen, High-dimensional interior crisis in the Kuramoto–Shivashinsky equation, *Phys. Rev. E* 65 (2002) 035203.
- [75] E.L. Rempel, A.C. Chian, High-dimensional chaotic saddles in the Kuramoto–Shivashinsky equation, *Phys. Lett. A* 319 (2003) 104–109.
- [76] E.L. Rempel, A.C. Chian, E.E. Macau, R.R. Rosa, Analysis of chaotic saddles in high-dimensional dynamical systems: The Kuramoto–Shivashinsky equation, *Chaos* 14 (2004) 545–556.
- [77] E.L. Rempel, A.C. Chian, Intermittency induced by attractor-merging crisis in the Kuramoto–Shivashinsky equation, *Phys. Rev. E* 71 (2005) 016203.
- [78] H. Nusse, J. Yorke, A procedure for finding numerical trajectories on chaotic saddles, *Physica D* 36 (1989) 137–156.
- [79] K. Szabó, T. Tél, Thermodynamics of attractor enlargement, *Phys. Rev. E* 50 (1994) 1070–1082.
- [80] K. Szabó, T. Tél, Transient chaos as the backbone of dynamics on strange attractors beyond crisis, *Phys. Lett. A* 196 (1994) 173–180.
- [81] K.G. Szabó, Y.-C. Lai, T. Tél, C. Grebogi, Critical exponents for gap-filling at crisis, *Phys. Rev. Lett.* 77 (1996) 3102–3105.
- [82] K.G. Szabó, Y.-C. Lai, T. Tél, C. Grebogi, Topological scaling and gap filling at crises, *Phys. Rev. E* 61 (2000) 5019–5032.
- [83] E.L. Rempel, A.C. Chian, Origin of transient and intermittent dynamics in spatiotemporal chaotic systems, *Phys. Rev. Lett.* 98 (2007) 014101.
- [84] Kaifen He, A.C.-L. Chian, Critical dynamic events at the crisis of transition to spatiotemporal chaos, *Phys. Rev. E* 69 (2004) 026207.
- [85] J. Sommerer, W. Ditto, C. Grebogi, E. Ott, M. Spano, Experimental confirmation of the scaling theory for noise-induced crises, *Phys. Rev. Lett.* 66 (1991) 1947–1950.
- [86] E.L. Rempel, A.C. Chian, R.A. Miranda, Chaotic saddles at the onset of intermittent spatiotemporal chaos, *Phys. Rev. E* 76 (2007) 056217.
- [87] Y.-C. Lai, R.L. Winslow, Riddled parameter space in spatiotemporal chaotic dynamical systems, *Phys. Rev. Lett.* 72 (1994) 1640–1643.
- [88] Y.-C. Lai, R.L. Winslow, Fractal basin boundaries in coupled map lattices, *Phys. Rev. E* 50 (1994) 3470–3473.
- [89] Y.-C. Lai, R.L. Winslow, Extreme sensitive dependence on parameters and initial conditions in spatio-temporal chaotic dynamical systems, *Physica D* 74 (1994) 353–371.
- [90] H. Kantz, P. Grassberger, Repellers, semi-attractors, and long-lived chaotic transients, *Physica D* 17 (1985) 75–86.
- [91] K. Falconer, *The Geometry of Fractal Sets*, Cambridge University Press, Cambridge, 1985.

- [92] B.R. Hunt, E. Ott, J.A. Yorke, Fractal dimensions of chaotic saddles of dynamical systems, *Phys. Rev. E* 54 (1996) 4819–4823.
- [93] G. Giacomelli, S. Lepri, A. Politi, Statistical properties of bidimensional patterns generated from delayed and extended maps, *Phys. Rev. E* 51 (1995) 3939–3944.
- [94] S. Grossmann, The onset of shear flow turbulence, *Rev. Modern Phys* 72 (2000) 603–618.
- [95] B. Eckhardt, T.M. Schneider, B. Hof, J. Westerweel, Turbulence in pipe flows, *Annu. Rev. Fluid. Mech.* 39 (2007) 447–468.
- [96] U. Brosa, Turbulence without strange attractor, *J. Stat. Phys.* 55 (1989) 1303–1312.
- [97] J. Peixinho, T. Mullin, Decay of turbulence in pipe flow, *Phys. Rev. Lett.* 96 (2006) 094501.
- [98] J.D. Skufca, J.A. Yorke, B. Eckhardt, Edge of chaos in a parallel shear flow, *Phys. Rev. Lett.* 96 (2006) 174101.
- [99] T.M. Schneider, B. Eckhardt, J.A. Yorke, Turbulence transition and the edge of chaos in pipe flow, *Phys. Rev. Lett.* 99 (2007) 034502.
- [100] B. Hof, C.W.H. Dorne, J. Westerweel, F.T.M. Nieuwstadt, H. Faisst, Experimental observation of nonlinear traveling wave in turbulent pipe flow, *Science* 305 (2004) 1594–1598.
- [101] T.M. Schneider, B. Eckhardt, J. Vollmer, Statistical analysis of coherent structures in transitional pipe flows, *Phys. Rev. E* 75 (2007) 066313.
- [102] J.F. Gibson, J. Halcrow, P. Cvitanovic, Visualizing the geometry of state space in plane couette flow, 2007, [arXiv:0705.3957](https://arxiv.org/abs/0705.3957).
- [103] B. Eckhardt, Turbulence transition in pipe flow: Some open questions, *Nonlinearity* 21 (2008) T1–T11.
- [104] R. Artuso, E. Aurell, P. Cvitanovic, Recycling of strange sets. 1. Cycle expansions, *Nonlinearity* 3 (2) (1990) 325–359.
- [105] R. Artuso, E. Aurell, P. Cvitanovic, Recycling of strange sets. 2. Applications, *Nonlinearity* 3 (2) (1990) 361–386.
- [106] F. Waleffe, Three-dimensional coherent states in plane shear flows, *Phys. Rev. Lett.* 81 (1998) 4140–4143.
- [107] A. Schmiegél, B. Eckhardt, Fractal stability border in plane Couette flow, *Phys. Rev. Lett.* 79 (1997) 5250–5253.
- [108] T.M. Schneider, M. Lagha, F. De Lillo, B. Eckhardt, Laminar-turbulent boundary in plane Couette flow, 2007. Preprint.
- [109] B. Eckhardt, H. Faisst, A. Schmiegél, T.M. Schneider, Dynamical systems and the transition to turbulence in linearly stable shear flows, *Phyl. Trans. Roy. Soc.* 366 (2008) 1297–1315.
- [110] H. Fujisaka, K. Egami, T. Yamada, Glassy dynamics in a spatially distributed dynamical system, *Phys. Lett.* 174 (1993) 103–110.
- [111] D.B. Vasconcelos, R.L. Viana, S.R. Lopes, S.E.de S. Pinto, Conversion of local transient chaos into global laminar states in coupled map lattices with long-range interactions, *Physica A* 367 (2006) 158–172.
- [112] L.M. Pecora, T.L. Carroll, Master stability functions for synchronized coupled systems, *Phys. Rev. Lett.* 80 (1998) 2109–2112.
- [113] A. Pikovsky, M. Rosenblum, J. Kurths, Synchronization. A Universal Concept in Nonlinear Science, Cambridge University Press, Cambridge, 2001.
- [114] M. Antoni, S. Ruffo, Clustering and relaxation in hamiltonian long-range dynamics, *Phys. Rev. E* 52 (1995) 2361–2374.
- [115] A. Pluchino, V. Latora, A. Rapisarda, Metastable states, anomalous distributions and correlations in the hmf model, *Physica D* 193 (2004) 315–328.
- [116] Y.Y. Yamaguchi, J. Barré, F. Bouchet, T. Dauxois, S. Ruffo, Stability criteria of the vlasov equation and quasi-stationary states of the hmf model, *Physica A* 337 (2004) 36–66.
- [117] E. Altmann, H. Kantz, Hypothesis of strong chaos and anomalous diffusion in coupled symplectic maps, *Europhys. Lett.* 78 (2007) 10008.
- [118] H. Morita, K. Kaneko, Collective oscillation in a Hamiltonian system, *Phys. Rev. Lett.* 96 (2006) 050602.
- [119] A.P.S. de Moura, Strange nonchaotic repellers, *Phys. Rev. E* 76 (2007) 036218.
- [120] U. Feudel, S. Kuznetsov, A. Pikovsky, *Strange Nonchaotic Attractors*, World Scientific, Singapore, 2006.
- [121] H.W. Yin, J.D. Dai, H.J. Zhang, Average lifetime and geometric properties for superlong transients in a hybrid optical bistable system, *Phys. Rev. E* 54 (1996) 371–375.
- [122] M. Dhamala, Y.-C. Lai, R.D. Holt, How often are chaotic transients in spatially extended ecological systems? *Phys. Lett.* 280 (2001) 297–302.
- [123] P. Brunet, L. Limat, Defects and spatiotemporal disorder in a pattern of falling liquid columns, *Phys. Rev. A* 70 (2004) 046207.